(1–180) did not. The Tax–CDC37(1–200) complex was translocated to the nucleus, whereas Tax–CDC37(1–378; wild type) stayed in the cytoplasm (Figure 4d). Collectively, these findings suggested the direct involvement of CDC37 for Tax stabilization.

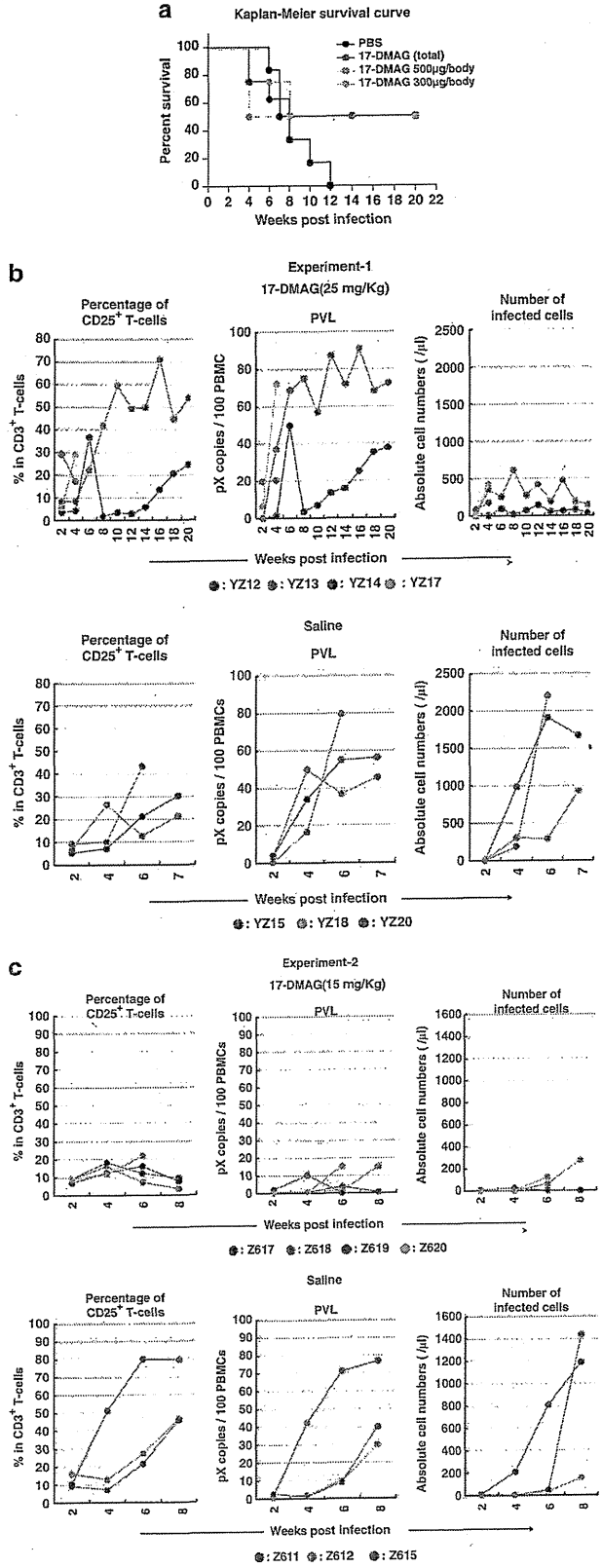

An oral administration of 17-DMAG to ATL model mice induced blockade of aggressive proliferation and multiple tissue invasions of transformed lymphocytes and improved survival rate

The demonstration that 17-DMAG has profound effects on Tax stability and the fact that it is water soluble suggested that this compound could be tested in a recently developed preclinical model of ATL.[23,28]

SCID mice were injected with 2×10^6 Lck-Tax cells intraperitoneally and treated for 5 consecutive days per week for 2 weeks with saline alone or with 17-DMAG in saline at 5 or 15 mg/kg. Mice were euthanized 21 days after cell inoculation. The blood smear indicated apparent reduction of Lck-Tax cells with increasing doses of 17-DMAG to saline controls (Figures 5a, e and i), although the quantitative cell counts were not obtained. The white pulp in greatly enlarged spleens (splenomegaly) of control mice was markedly expanded with red pulp compression (Figure 5b), and the livers and lungs of saline control mice were characterized by extensive perivascular infiltrations with Lck-Tax cells (Figures 5c and d). These pathologies were progressively reduced in mice treated with 17-DMAG (spleen, Figures 5f and j; liver, Figures 5g and k; and lung, Figures 5h and l).

We then determined the survival improvement through 17-DMAG oral administration with another preclinical ATL model (Figure 6). Each 7 (14 in total) huNOG mice[28] were injected with 1×10^6 HTLV-1-producing JEX cells (details are described in Supplementary Information), and 2 weeks after inoculation, each 4 of these mice (8 in total) were treated 20 times with 15 or 25 mg/kg of 17-DMAG for 4 weeks (as shown in Supplementary Figure 4), whereas the remaining 6 mice received saline only. The percentage of CD25-positive T cells, proviral load and the number of human leukocytes in peripheral blood were monitored. Four of eight 17-DMAG-treated mice died within 8 weeks post inoculation probably because of high drug dosage, but other four mice (50%) survived more than 20 weeks, whereas all the saline-treated controls died within 12 weeks post inoculation. The average survival period of controls and 17-DMAG-treated subjects were 8.33 and 14.75 weeks, respectively. However, the survival periods of 17-DMAG-treated subjects could be extended because four subjects were sacrificed at 24 weeks post inoculation for pathological examination (Supplementary Figure 4). The numbers of HTLV-1-infected human leukocytes in peripheral blood of 17-DMAG-treated subjects were also 5–10 times fewer than those of saline controls (Figures 6b and c).

Additive effects for growth arrest and apoptosis induction by concomitant 17-DMAG/Nutlin-3a treatment against ATL cells

The standard chemotherapy against ATL, named as leukemia study group 15 (LSG15), is currently employing the combination of four different anticancer drugs that frequently brings serious side effects to patients.[40] We previously demonstrated that a novel MDM-2-antagonizing/p53-stabilizing drug, Nutlin-3a, induces

Figure 6. Improved survival and suppression of the growth of HTLV-1-infected T cells by 17-DMAG oral treatment. (**a**) Kaplan–Meier survival curve of HTLV-1-infected huNOG mice. All mice have reconstituted human immune system by the transplantation of hematopoietic stem cells (huNOG) and have received 1 million JEX cells, which produce HTVL-1 infectious virus (see the details in Supplementary Figure 4). JEX/huNOG mice received 17-DMAG by oral administration for 4 weeks (2–6 weeks post inoculation, five times/week) at the dosage of 25 mg/kg (orange line) and 15 mg/kg (pink line). Control mice received the same volume of PBS. (**b**) The percentage of CD25-positive T cells, PVL and the number of HTLV-1-infected cells in peripheral blood of infected mice are shown. Upper panel represents the results from 17-DMAG-treated (25 mg/kg) mice; lower panel represents those of control mice. (**c**) Same experiments with 17-DMAG (15 mg/kg, upper panel) and PBS control (lower panel). PBS, phosphate buffered saline; PVL, proviral load.

the senescent death to ATL cells.[41] We then examined the additive anti-ATL effects of 17-DMAG and Nutlin-3a. Suboptimal dose of 17-DMAG (0.1 μM) or Nutlin-3a (1 μM) alone did not induce sufficient apoptotic or growth-arrest activities to ATL cell lines. However, the combined use of both induced significant growth suppressive and apoptotic properties (Figure 7), suggesting the possible combinational use of these drugs for further clinical studies.

DISCUSSION

HTLV-1 is the etiologic agent of ATL. Current studies indicate that worldwide there are more than 20 million HTLV-1 carriers and that 5% of these carriers will develop ATL.[42] The current standard for treatment of acute- or lymphoma-type ATL in Japan is CHOP or its modified regimen LSG15; however, the responses to this treatment regimen are limited to 31.1% of patients with 2-year survivals.[40] As malignant cells from relapsed patients are also resistant to other chemotherapeutic interventions, novel strategies for treatment of ATL are urgently required.

In this study, we demonstrated the significant inhibitory effects of 17-DMAG on Tax-mediated NF-κB signaling *in vitro* and *ex vivo*. The most striking observations obtained *in vitro* were (a) 17-DMAG-induced Tax degradation that resulted from inhibiting the formation of the Tax–IKK–HSP90/CDC37 ternary complex (Figures 1a–d); (b) induction of growth suppression and apoptosis of ATL cells while having little or no effect on normal PBLs (Figures 2a and b). We also found that the stability of Tax was heavily dependent on the CBD of CDC37 (Figures 4a and b). GA-dependent NF-κB downregulation in ATL cells was reported, and inhibition of autophagic activity seemed to affect the conversion of p100 (NF-κB2 precursor) to active p52.[32] We observed this time 17-DMAG-dependent Tax degradation and its blockade by AICAR and 3-MA (autophagy inhibitors) but not by the proteasome inhibitor MG-132 (Figure 1d), suggesting the direct involvement of the autophagosome on Tax metabolism in cells. This issue should further be investigated with ubiquitylation-deficient mutants Tax[24,31] or the autophagy-deficient cells.[43,44]

The CBD of CDC37 has been reported to bind preferentially to a specific glycine-rich motif — GXGXXG.[45] Indeed, Tax has a similar motif in its N terminus. CBD played crucial roles in stabilizing Tax and Tax–CDC37 complex formation (Figures 4c and d). CBD-containing mutants of CDC37 seemed to enhance the machinery responsible for Tax degradation as we did not detect any decrease in Tax levels in response to an siRNA knockdown of CDC37 (Supplementary Figure 5). Interestingly, the Tax-destabilizing CDC37(N200) translocated Tax to the nucleus, whereas wild-type CDC37 stayed with Tax in the cytoplasm (Figure 4d), and it implies that this translocation could be related to the Tax destabilization. For the future, it would be worth trying to identify a chemical compound that mimics the structure of CBD and could function as an inducer of Tax degradation. HSP90 and its co-chaperone's involvement in multiple signaling cascades, especially, in cancer cells, has been reported.[46,47] Indeed, 17-DMAG also suppressed NF-κB signaling mediated by other activators NIK, MEKK1, AKT, TAB2 and IKKα/β (data not shown). We also found that 17-DMAG treatment induced Tax degradation; potentially 17-DMAG treatment may also have led to the destabilization of other NF-κB signaling activators.

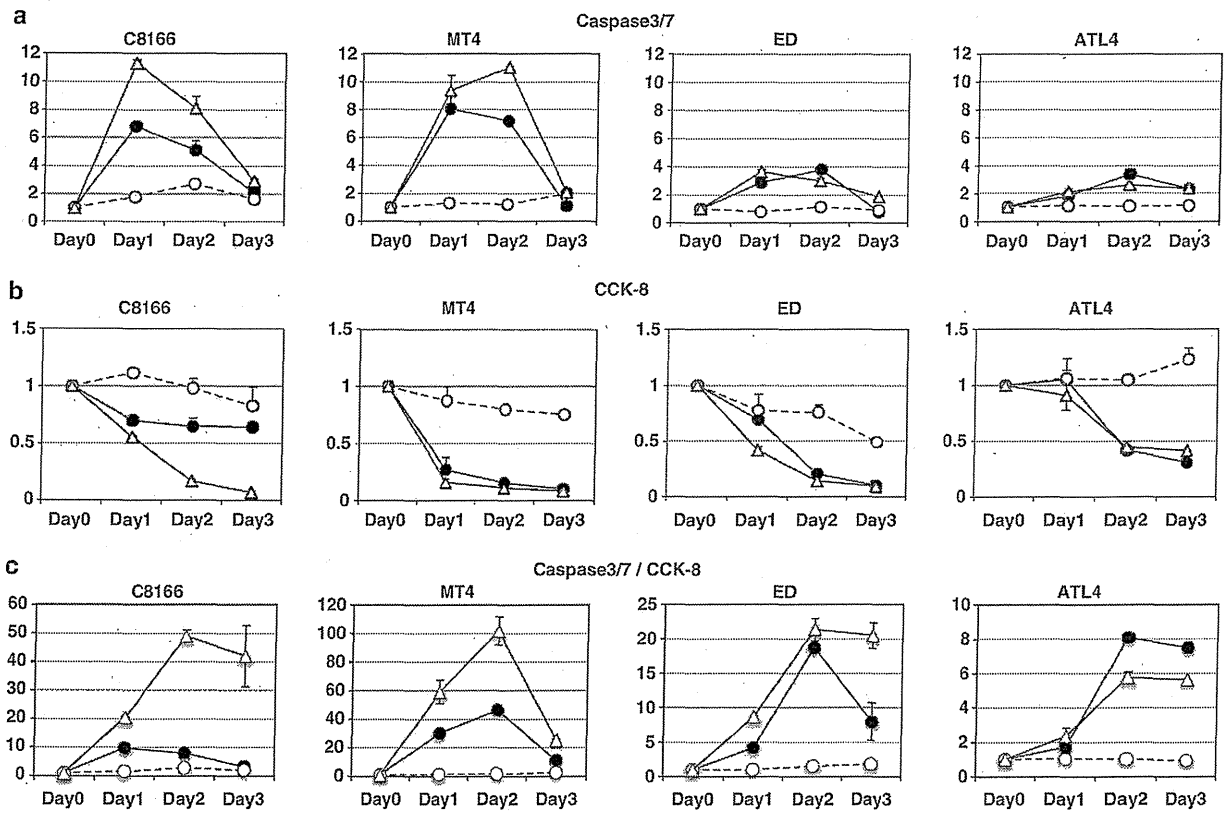

Figure 7. Additive anti-ATL cell effects by the combined dosage of 17-DMAG and Nutlin-3a. (**a**) ATL cell lines C8166, MT4, ED and ATL4 were treated with either suboptimal single dose of 17-DMAG (0.1 μM, black circles) and Nutlin-3a (1 μM, white circles)[41] or both (white triangles) for 3 days and harvested for caspase-3/7 assays (**a**) or CCK-8 assays (**b**) as described in Figure 2. Each untreated cell's value was set as 1. (**c**) Each caspase-3/7 (apoptotic) value was divided by CCK-8 (growth arrest) value to manifest the additive effects (see the Discussion section). CCK-8, Cell Counting Kit 8.

We have determined the therapeutic effects of 17-DMAG on two different ATL model systems through its oral administration. First, we tested 17-DMAG induced prevention of Lck-Tax infiltration in SCID mice, and 5 and 15 mg/kg of oral administration of 17-DMAG for 2 weeks reduced 74% and 83% of Lck-Tax cells, respectively; splenomegaly or massive infiltration of Lck-Tax cells into livers and lungs was also significantly reduced (Figure 5). In all experiments, 17-DMAG mice did not show any body weight losses or inactiveness compared with saline controls.

We then switched to another ATL model experiment JEX/huNOG, which has humanized immune environment in NOG mice and has inoculated HTLV-1-producing Jurkat cells. With oral administration of both 15 and 25 mg/kg 17-DMAG to JEX/huNOG, four of eight mice survived more than 20 weeks, whereas saline controls died within 12 weeks (Figure 6a). 17-DMAG treatment also reduced the number of HTLV-1-infected cells in peripheral blood, suggesting that 17-DMAG treatment could intervene the clonal T-cell development to ATL (Figure 6b). Although this preliminary experiment did not provide statistically significant survival rates, efficacy of this treatment is indeed highly expected. It is necessary to find the optimized conditions suppressing the ATL cell proliferation without any serious side effects.

Tax has pleiotropic effects on intra-cellular or inter-cellular signalings including mitotic checkpoint disruption,[48] aberrant cell-cycle progression[49,50] and altered chemotaxis.[51] The present ATL treatment protocols target the cytoskeletons or DNA replications with multiple doses of anticancer drugs (called as LSG15), and significant side effects by this treatment have been frequently recognized.[40] We have recently demonstrated the potential uses of molecularly targeted inhibitors of ATL cell proliferation, such as a MDM-2 ubiquitin ligase inhibitor Nutlin-3a[41] or CXCR4 antagonist AMD3100.[51] Nutlin-3a induces growth arrest and senescent-cell death of ATL cells at the 10 μM concentration, but normal PBLs are also significantly affected.[41] The combined use of 17-DMAG (0.1 μM) and Nutlin-3a (1 μM), suboptimal concentration for single use, significantly enhanced both apoptotic and growth suppressive effects (Figures 7a and b). This concurrent effects can be manifested with the division of caspase-3/7 values by Cell Counting Kit 8 values (Figure 7c). Besides Nutlin-3a, we also tested the efficacy of 17-DMAG plus LSG15 (without predonisolone; Supplementary Figure 6). Unlike the results of 17-DMAG/Nutlin-3a, 17-DMAG/LSG15 did not show any clear additive effects probably because LSG15 affects cell-cycle progression with a wide range of spectrum, but the effects of Nutlin-3a are specifically restricted to p53 stabilization.

It remains to be seen whether 17-DMAG is effective for ATL patients' treatment; elsewhere Hertlein *et al.*[52] have reported 17-DMAG's clinical application against chronic lymphocytic leukemia. Perhaps in future studies, 17-DMAG and other new drugs with novel anti-ATL activities such as Nutlin-3a, AMD3100 or a monoclonal anti-CCR4 antibody (KW-0761)[53] will provide more effective and less toxic ATL therapy.

CONFLICT OF INTEREST

The authors declare no conflict of interest.

ACKNOWLEDGEMENTS

We are indebted to Dr Herbert C Morse III for his helpful discussion and comments. We thank Mr T Kawashima and Ms Y Itoh for technical assistance and Drs K Terasawa, C Pique and K Nagata for providing plasmid DNAs. EI was a research fellow of the Okinawa Science and Technology Promotion Center. This study was supported in part by grants from the Ministry of Education, Culture, Sports, Science and Technology; the Ministry of Health, Labor and Welfare; the Ministry of Economy, Trade and Industry; Japan Science and Technology Agency; Okinawa Science and Technology Promotion Center; and Miyazaki Prefectural Industrial Support Foundation.

AUTHOR CONTRIBUTIONS

HI, J-IF and HdH designed the research; HdH, HS, WWH, KT, TU and J-IF developed the ATL animal model; EI, AK, KT, ST, SH, TMa, TU, TMi, KS, J-IF, HdH and HI performed the research; AN, MH, HrH, YY, YT, HS, WH, YM, KTJ, MO and KM contributed new reagents/materials; AK, KT, J-IF and HdH contributed pathologic analysis; and EI, KT, J-IF, HdH and HI wrote the paper.

REFERENCES

1 Li Q, Verma IM. NF-kappaB regulation in the immune system. *Nat Rev Immunol* 2002; **2**: 725–734.
2 Janssens S, Tschopp J. Signals from within: the DNA-damage-induced NF-kappaB response. *Cell Death Differ* 2006; **13**: 773–784.
3 Karin M. NF-kappaB as a critical link between inflammation and cancer. *Cold Spring Harb Perspect Biol* 2009; **1**: a000141.
4 Hayden MS, Ghosh S. Shared principles in NF-kappaB signaling. *Cell* 2008; **132**: 344–362.
5 Li XH, Fang X, Gaynor RB. Role of IKK-gamma/NEMO in assembly of the I-kappaB kinase complex. *J Biol Chem* 2001; **276**: 4494–4500.
6 Li Q, Van Antwerp D, Mercurio F, Lee KF, Verma IM. Severe liver degeneration in mice lacking the I-kappaB kinase 2 gene. *Science* 1999; **284**: 321–325.
7 Schmidt-Supprian M, Bloch W, Courtois G, Addicks K, Israel A, Rajewsky K *et al.* NEMO/IKK-gamma-deficient mice model incontinentia pigmenti. *Mol Cell* 2000; **5**: 981–992.
8 Li Q, Lu Q, Hwang JY, Buscher D, Lee KF, Izpisua-Belmonte JC *et al.* IKK1-deficient mice exhibit abnormal development of skin and skeleton. *Genes Dev* 1999; **13**: 1322–1328.
9 Takeda K, Takeuchi O, Tsujimura T, Itami S, Adachi O, Kawai T *et al.* Limb and skin abnormalities in mice lacking IKK-alpha. *Science* 1999; **284**: 313–316.
10 Yamaoka S, Courtois G, Bessia C, Whiteside ST, Weil R, Agou F *et al.* Complementation cloning of NEMO, a component of the I-kappaB kinase complex essential for NF-kappaB activation. *Cell* 1998; **93**: 1231–1240.
11 Iha H, Kibler KV, Yedavalli VR, Peloponese JM, Haller K, Miyazato A *et al.* Segregation of NF-kappaB activation through NEMO/IKK-gamma by Tax and TNF-alpha: implications for stimulus-specific interruption of oncogenic signaling. *Oncogene* 2003; **22**: 8912–8923.
12 Chen G, Cao P, Goeddel DV. TNF-induced recruitment and activation of the IKK complex require Cdc37 and Hsp90. *Mol Cell* 2002; **9**: 401–410.
13 Bouwmeester T, Bauch A, Ruffner H, Angrand PO, Bergamini G, Croughton K *et al.* A physical and functional map of the human TNF-alpha/NF-kappa B signal transduction pathway. *Nat Cell Biol* 2004; **6**: 97–105.
14 Yoshida M. Multiple viral strategies of HTLV-1 for dysregulation of cell growth control. *Annu Rev Immunol* 2001; **19**: 475–496.
15 Hall WW, Fujii M. Deregulation of cell-signaling pathways in HTLV-1 infection. *Oncogene* 2005; **24**: 5965–5975.
16 Matsuoka M, Jeang KT. Human T-cell leukaemia virus type 1 (HTLV-1) infectivity and cellular transformation. *Nat Rev Cancer* 2007; **7**: 270–280.
17 Jin DY, Giordano V, Kibler KV, Nakano H, Jeang KT. Role of adapter function in oncoprotein-mediated activation of NF-kappaB. Human T-cell leukemia virus type I Tax interacts directly with I-kappaB kinase gamma. *J Biol Chem* 1999; **274**: 17402–17405.
18 Carter RS, Pennington KN, Ungurait BJ, Ballard DW. *In vivo* identification of inducible phosphoacceptors in the IKK-gamma/NEMO subunit of human I-kappaB kinase. *J Biol Chem* 2003; **278**: 19642–19648.
19 Lamsoul I, Lodewick J, Lebrun S, Brasseur R, Burny A, Gaynor RB *et al.* Exclusive ubiquitination and sumoylation on overlapping lysine residues mediate NF-kappaB activation by the human T-cell leukemia virus Tax oncoprotein. *Mol Cell Biol* 2005; **25**: 10391–10406.
20 Chu ZL, DiDonato JA, Hawiger J, Ballard DW. The Tax oncoprotein of human T-cell leukemia virus type 1 associates with and persistently activates I-kappaB kinases containing IKK-alpha and IKK-beta. *J Biol Chem* 1998; **273**: 15891–15894.
21 Geleziunas R, Ferrell S, Lin X, Mu Y, Cunningham Jr ET, Grant M *et al.* Human T-cell leukemia virus type 1 Tax induction of NF-kappaB involves activation of the I-kappaB kinase alpha (IKK-alpha) and IKK-beta cellular kinases. *Mol Cell Biol* 1998; **18**: 5157–5165.
22 Egorin MJ, Lagattuta TF, Hamburger DR, Covey JM, White KD, Musser SM *et al.* Pharmacokinetics, tissue distribution, and metabolism of 17-(dimethylaminoethylamino)-17-demethoxygeldanamycin (NSC 707545) in CD2F1 mice and Fischer 344 rats. *Cancer Chemother Pharmacol* 2002; **49**: 7–19.
23 Hasegawa H, Sawa H, Lewis MJ, Orba Y, Sheehy N, Yamamoto Y *et al.* Thymus-derived leukemia–lymphoma in mice transgenic for the Tax gene of human T-lymphotropic virus type I. *Nat Med* 2006; **12**: 466–472.

24 Chiari E, Lamsoul I, Lodewick J, Chopin C, Bex F, Pique C. Stable ubiquitination of human T-cell leukemia virus type 1 tax is required for proteasome binding. *J Virol* 2004; **78:** 11823–11832.
25 Momose F, Naito T, Yano K, Sugimoto S, Morikawa Y, Nagata K. Identification of Hsp90 as a stimulatory host factor involved in influenza virus RNA synthesis. *J Biol Chem* 2002; **277:** 45306–45314.
26 Terasawa K, Minami Y. A client-binding site of Cdc37. *FEBS J* 2005; **272:** 4684–4690.
27 Ueyama T, Kusakabe T, Karasawa S, Kawasaki T, Shimizu A, Son J *et al.* Sequential binding of cytosolic Phox complex to phagosomes through regulated adaptor proteins: evaluation using the novel monomeric Kusabira-Green system and live imaging of phagocytosis. *J Immunol* 2008; **181:** 629–640.
28 Nie C, Sato K, Misawa N, Kitayama H, Fujino H, Hiramatsu H *et al.* Selective infection of CD4+ effector memory T lymphocytes leads to preferential depletion of memory T lymphocytes in RS HIV-1-infected humanized NOD/SCID/IL-2Rgammanull mice. *Virology* 2009; **394:** 64–72.
29 Ueno S, Umeki K, Takajo I, Nagatomo Y, Kusumoto N, Umekita K *et al.* Proviral loads of human T-lymphotropic virus type 1 in asymptomatic carriers with different infection routes. *Int J Cancer* 2012; **130:** 2318–2326.
30 De Valck D, Jin DY, Heyninck K, Van de Craen M, Contreras R, Fiers W *et al.* The zinc finger protein A20 interacts with a novel anti-apoptotic protein which is cleaved by specific caspases. *Oncogene* 1999; **18:** 4182–4190.
31 Peloponese JM, Iha H, Yedavalli VR, Miyazato A, Li Y, Haller K *et al.* Ubiquitination of human T-cell leukemia virus type 1 tax modulates its activity. *J Virol* 2005; **78:** 11686–11695.
32 Yan P, Qing G, Qu Z, Wu CC, Rabson A, Xiao G. Targeting autophagic regulation of NFkappaB in HTLV-I transformed cells by geldanamycin: implications for therapeutic interventions. *Autophagy* 2007; **3:** 600–603.
33 Mitsiades CS, Mitsiades NS, McMullan CJ, Poulaki V, Kung AL, Davies FE *et al.* Antimyeloma activity of heat shock protein-90 inhibition. *Blood* 2006; **107:** 1092–1100.
34 Jeang KT, Chiu R, Santos E, Kim SJ. Induction of the HTLV-I LTR by Jun occurs through the Tax-responsive 21-bp elements. *Virology* 1991; **181:** 218–227.
35 Prodromou C, Roe SM, O'Brien R, Ladbury JE, Piper PW, Pearl LH. Identification and structural characterization of the ATP/ADP-binding site in the Hsp90 molecular chaperone. *Cell* 1997; **90:** 65–75.
36 Meyer P, Prodromou C, Hu B, Vaughan C, Roe SM, Panaretou B *et al.* Structural and functional analysis of the middle segment of hsp90: implications for ATP hydrolysis and client protein and cochaperone interactions. *Mol Cell* 2003; **11:** 647–658.
37 Minami Y, Kimura Y, Kawasaki H, Suzuki K, Yahara I. The carboxy-terminal region of mammalian HSP90 is required for its dimerization and function *in vivo*. *Mol Cell Biol* 1994; **14:** 1459–1464.
38 Roe SM, Ali MM, Meyer P, Vaughan CK, Panaretou B, Piper PW *et al.* The mechanism of Hsp90 regulation by the protein kinase-specific cochaperone p50(cdc37). *Cell* 2004; **116:** 87–98.
39 Silverstein AM, Grammatikakis N, Cochran BH, Chinkers M, Pratt WB. p50(cdc37) binds directly to the catalytic domain of Raf as well as to a site on hsp90 that is topologically adjacent to the tetratricopeptide repeat binding site. *J Biol Chem* 1998; **273:** 20090–20095.
40 Uozumi K. Treatment of adult T-cell leukemia. *J Clin Exp Hematop* 2010; **50:** 9–25.
41 Hasegawa H, Yamada Y, Iha H, Tsukasaki K, Nagai K, Atogami S *et al.* Activation of p53 by Nutlin-3a, an antagonist of MDM2, induces apoptosis and cellular senescence in adult T-cell leukemia cells. *Leukemia* 2009; **23:** 2090–2101.
42 Proietti FA, Carneiro-Proletti AB, Catalan-Soares BC, Murphy EL. Global epidemiology of HTLV-I infection and associated diseases. *Oncogene* 2005; **24:** 6058–6068.
43 Mizushima N, Yoshimori T, Ohsumi Y. The role of Atg proteins in autophagosome formation. *Annu Rev Cell Dev Biol* 2011; **27:** 107–132.
44 Codogno P, Mehrpour M, Proikas-Cezanne T. Canonical and non-canonical autophagy: variations on a common theme of self-eating? *Nat Rev Mol Cell Biol* 2011; **13:** 7–12.
45 Terasawa K, Yoshimatsu K, Iemura SI, Natsume T, Tanaka K, Minami Y. Cdc37 interacts with the glycine-rich loop of Hsp90 client kinases. *Mol Cell Biol* 2006; **26:** 3378–3389.
46 Calderwood SK, Khaleque MA, Sawyer DB, Ciocca DR. Heat shock proteins in cancer: chaperones of tumorigenesis. *Trends Biochem Sci* 2006; **31:** 164–172.
47 Caplan AJ, Mandal AK, Theodoraki MA. Molecular chaperones and protein kinase quality control. *Trends Cell Biol* 2007; **17:** 87–92.
48 Jin DY, Spencer F, Jeang KT. Human T cell leukemia virus type 1 oncoprotein Tax targets the human mitotic checkpoint protein MAD1. *Cell* 1998; **93:** 81–91.
49 Giam CZ, Jeang KT. HTLV-1 Tax and adult T-cell leukemia. *Front Biosci* 2007; **12:** 1496–1507.
50 Tanaka Y. Activation of leukocyte function-associated antigen-1 on adult T-cell leukemia cells. *Leuk Lymphoma* 1999; **36:** 15–23.
51 Kawaguchi A, Orba Y, Kimura T, Iha H, Ogata M, Tsuji T *et al.* Inhibition of the SDF-1alpha-CXCR4 axis by the CXCR4 antagonist AMD3100 suppresses the migration of cultured cells from ATL patients and murine lymphoblastoid cells from HTLV-I Tax transgenic mice. *Blood* 2009; **114:** 2961–2968.
52 Hertlein E, Wagner AJ, Jones J, Lin TS, Maddocks KJ, Towns III WH *et al.* 17-DMAG targets the nuclear factor-kappaB family of proteins to induce apoptosis in chronic lymphocytic leukemia: clinical implications of HSP90 inhibition. *Blood* 2010; **116:** 45–53.
53 Yamamoto K, Utsunomiya A, Tobinai K, Tsukasaki K, Uike N, Uozumi K *et al.* Phase I study of KW-0761, a defucosylated humanized anti-CCR4 antibody, in relapsed patients with adult T-cell leukemia–lymphoma and peripheral T-cell lymphoma. *J Clin Oncol* 2010; **28:** 1591–1598.

Supplementary Information accompanies this paper on the Blood Cancer Journal website (http://www.nature.com/bcj).

Biochemical and Biophysical Research Communications 441 (2013) 102–107

Contents lists available at ScienceDirect

Biochemical and Biophysical Research Communications

journal homepage: www.elsevier.com/locate/ybbrc

Suppressed expression of *NDRG2* correlates with poor prognosis in pancreatic cancer

Akihiro Yamamura [a,b], Koh Miura [a], Hideaki Karasawa [a], Kazuhiro Morishita [c], Keiko Abe [b], Yasuhiko Mizuguchi [b], Yuriko Saiki [b], Shinichi Fukushige [b], Naoyuki Kaneko [a], Tomohiko Sase [a], Hiroki Nagase [d], Makoto Sunamura [a,b,e], Fuyuhiko Motoi [a], Shinichi Egawa [a], Chikashi Shibata [a], Michiaki Unno [a], Iwao Sasaki [a], Akira Horii [b,*]

[a] Department of Surgery, Tohoku University, Graduate School of Medicine, Sendai, Japan
[b] Department of Pathology, Tohoku University, Graduate School of Medicine, Sendai, Japan
[c] Department of Medical Sciences, Faculty of Medicine, University of Miyazaki, Miyazaki, Japan
[d] Department of Advanced Medical Science, Nihon University School of Medicine, Tokyo, Japan
[e] Department of Digestive Tract Surgery and Transplantation Surgery, Tokyo Medical University, Hachioji Medical Center, Tokyo, Japan

ARTICLE INFO

Article history:
Received 2 October 2013
Available online 14 October 2013

Keywords:
NDRG2
Epigenetic silencing
Hypermethylation
Pancreatic cancer
Prognostic factor

ABSTRACT

Pancreatic cancer is a highly lethal disease with a poor prognosis; the molecular mechanisms of the development of this disease have not yet been fully elucidated. N-myc downstream regulated gene 2 (*NDRG2*), one of the candidate tumor suppressor genes, is frequently downregulated in pancreatic cancer, but there has been little information regarding its expression in surgically resected pancreatic cancer specimens. We investigated an association between NDRG2 expression and prognosis in 69 primary resected pancreatic cancer specimens by immunohistochemistry and observed a significant association between poor prognosis and NDRG2-negative staining ($P = 0.038$). Treatment with trichostatin A, a histone deacetylase inhibitor, predominantly up-regulated *NDRG2* expression in the *NDRG2* low-expressing cell lines (PANC-1, PCI-35, PK-45P, and AsPC-1). In contrast, no increased *NDRG2* expression was observed after treatment with 5-aza-2′ deoxycytidine, a DNA demethylating agent, and no hypermethylation was detected in either pancreatic cancer cell lines or surgically resected specimens by methylation specific PCR. Our present results suggest that (1) *NDRG2* is functioning as one of the candidate tumor-suppressor genes in pancreatic carcinogenesis, (2) epigenetic mechanisms such as histone modifications play an essential role in *NDRG2* silencing, and (3) the expression of NDRG2 is an independent prognostic factor in pancreatic cancer.

1. Introduction

Pancreatic cancer is a highly lethal disease; few patients are diagnosed at a state early enough for curative treatments. It is the fourth most common cause of cancer death worldwide [1], and the long-term prognosis remain poor with a 5-year survival rate of less than 5% after the initial diagnosis [2]. One of the major hallmarks of pancreatic cancer is its extensive local tumor invasion and early systemic dissemination. The molecular basis for these characteristics of pancreatic cancer is incompletely understood.

N-Myc downstream regulated gene 2 (*NDRG2*) is a member of *NDRG* gene family that is highly expressed in many normal tissue types, including brain, spinal cord, skeletal muscle, heart, and salivary gland [3–5]. *NDRG* gene family members share 53–65% homologous amino acid sequences with each other. Each member has a distinct tissue specificity of expression and may be intimately involved in cell proliferation, differentiation, development, and stress responses [6].

NDRG2 has been reported to be a candidate tumor suppressor gene, and its expression is downregulated in a number of primary tumors developed in organs of brain and meninges [4,7,8], liver [9,10], pancreas [10], esophagus [11], stomach [12], colorectum [6,13,14], kidney [6], thyroid [15], oral cavity [16], prostate [17], gallbladder [18], blood [19], and lung [20]. *NDRG2* is reported to

Abbreviations: *NDRG2*, N-myc downstream regulated gene 2; 5-aza-dC, 5-aza-2′ deoxycytidine; TSA, trichostatin A; qRT-PCR, quantitative reverse transcription polymerase chain reaction; cDNA, complementary DNA; AU, arbitrary unit; *B2M*, β2-microglobulin; MSP, methylation-specific PCR; HDAC, histone deacetylase.

* Corresponding author. Address: Department of Pathology, Tohoku University, Graduate School of Medicine, 2-1 Seiryo-machi, Aoba-ku, Sendai 980-8575, Japan. Fax: +81 22 717 8047.
E-mail address: horii@med.tohoku.ac.jp (A. Horii).

0006-291X/$ - see front matter © 2013 Elsevier Inc. All rights reserved.
http://dx.doi.org/10.1016/j.bbrc.2013.10.010

suppress proliferation and metastasis, and expressional inactivation of *NDRG2* may play an important role in carcinogenesis [4,9,11,12,21,22]. Several possible mechanisms, including promoter hypermethylation [7–9,13,16,23] and/or repression by MYC [4,11,14,15,24], are responsible for such expressional suppression. However, the precise mechanisms that lead to inactivation of *NDRG2* remain largely unknown, and role of *NDRG2* in human carcinogenesis is not yet well understood.

In the present study using immunohistochemistry, we found a significant association between poor prognosis and suppressed expression of NDRG2 in primary pancreatic cancer. Furthermore, *NDRG2* gene expression was up-regulated by histone deacetylase inhibitor in pancreatic cancer. It is notable that this histone modification has never previously been demonstrated in suppression of *NDRG2* expression in human cancer. These findings suggest that *NDRG2* is likely to be a novel prognostic marker and important indicator for a possible role of *NDRG2* in pancreatic cancer.

2. Materials and methods

2.1. Tissue specimens

A total of 69 pancreatic cancer tissues obtained from surgically resected specimens at Tohoku University Hospital (Sendai, Miyagi, Japan) during the period from 1997 to 2006 were analyzed. The clinical and histopathological characteristics of the pancreatic cancer patients are summarized in Table 1. Staging followed the TNM Classification of Malignant Tumor (6th edition) [25]. None of the patients had received any preoperative adjuvant therapy. The resected tissue specimens from these patients were fixed in 10% formalin and embedded in paraffin. Written informed consent was obtained from all patients. The study was approved by the Ethics Committee of Tohoku University School of Medicine.

Table 1
Relationship between NDRG2 expression and clinicopathological features of pancreatic cancer patients.

	NDRG2 expression		*P*-value
	Positive $n = 18$	Negative $n = 51$	
Gender			
Male	14	32	0.24
Female	4	19	
Age (mean, years)	61.2	64.0	0.25
Tumor size[a] (mm)	38.3	42.3	0.45
UICC Stage			
I	2	2	0.70
II	6	21	
III	6	16	
IV	4	12	
Differentiation			
Wel	2	1	0.14
Mod	15	41	
Por	1	9	
Lymph node metastasis			
N0	6	18	0.88
N1	12	33	
Lymphatic invasion			
Absent	3	5	0.61
Present	15	46	
Venous invasion			
Absent	0	4	0.22
Present	18	47	
Intrapancreatic neural invasion			
Absent	1	2	0.77
Present	17	49	

[a] Average longitudinal diameter.

2.2. Tissue array analysis and immunohistochemistry

A tissue array consisting of 69 paired pancreatic cancer and their corresponding normal tissues was constructed using TISSUE MICROPROCESSOR (AZUMAYA, Tokyo, Japan). Each paraffin-embedded block was cored out at a diameter of 3 mm, and the cored columns were re-embedded in paraffin. For further analyses, 4 μm slide sections were prepared. The immunohistochemical assay was done by the avidin–biotin–peroxidase method described previously [26]. Rabbit polyclonal anti-NDRG2 (1:3000, Atlas Antibodies AB, Stockholm, Sweden) and anti-rabbit (1:1000, Amersham Biosciences, Little Chalfont, UK) secondary antibodies were used. Immunoreactivity was evaluated by two pathologists. NDRG2 immmunoreactivity was detected in both the cytoplasm and the plasma membrane. Normal epithelial cells showed expression of NDRG2 in all specimens. NDRG2 immunoreactivity was defined by comparison the signal intensities of normal and cancerous tissues; strong, moderate, and weak designations denote signals with cancerous tissue that were stronger, similar, or weaker than the normal tissues, respectively. When no NDRG2 signal was detected, we defined the tumor as negative.

2.3. Cell lines analyzed in this study

Nine human pancreatic cancer cell lines (PANC-1, PCI-35, PK-45P, AsPC-1, BxPC-3, PK-1, MIAPaCa-2, PK8 and PK9) and two colorectal cancer cell lines (Clone A and LS174T) were used. These cell lines were also used in our previous studies and were maintained as described [27,28].

2.4. RNA and DNA extraction

Total RNAs from cultured cells were extracted using RNeasy Mini Kit (Qiagen, Valencia, CA), and their concentrations were determined using a NanoDrop ND-1000 Spectrophotometer (NanoDrop Technologies, Wilmington, DE). Genomic DNAs from cultured cells were extracted using DNeasy Blood & Tissue Kits (Qiagen) according to the manufacturer's instructions, and their concentrations were measured with a NanoDrop ND-1000 Spectrophotometer. All the processes were carried out according to the manufacturers' instructions.

2.5. Quantitative reverse transcription PCR (qRT-PCR)

Each aliquot of 2 μg total RNA was reverse transcribed to synthesize cDNA using a High Capacity cDNA Reverse Transcription Kit (Applied Biosystems, Foster City, CA) according to the manufacturer's instructions. qRT-PCR analyses were performed using an ABI PRISM 7000 Sequence Detection System (Applied Biosystems) following the manufacturer's instructions. Expression of β2-microglobulin (*B2M*) was used as the internal control [29]. The nucleotide sequences for primers, probes, and PCR conditions are listed in Table 2. Amplifications were carried out in the 15 μl reaction mixtures according to methods described previously [30]. The expression ratios of *NDRG2*/*B2M* were calculated and used for characterization. Each experiment was performed in triplicate.

2.6. 5-Aza-2′-deoxycytidine (5-aza-dC) and trichostatin A (TSA) treatment

Cells were seeded at a density of 2×10^6 cells per 100 mm dish and were maintained for 72 h while replacing the culture medium containing 1 μM 5-aza-dC (Sigma, St. Louis, MO) every 24 h. Subse-

Table 2
Nucleotide sequences of the primers and probes.

	Forward primer (5′–3′)	Reverse primer (5′–3′)	Probe (5′–3′)	Annealing temperature (°C)	PCR cycles	Product size (bp)
qRT-PCR						
NDRG2	GAAGATGCAGTGGTGGAATG	TCAGCTTGCCTGGCTGAGT	TTCCTCAAGATGGCTGACTCCGG	60	30	109
B2M[a]	TTTCAGCAAGGACTGGTCTTT	CCAAATGCGGCATCTTCAAAC	CTGAAAAAGATGAGTATGCCTGCCGTGTG	60	30	171
MSP						
Methylation specific primer	GTTTGCGGGAAGTTCGAGTC	CCGCCGACCCGACTAACG		70	35	134
Unmethylation specific primer	GTGGGTTTGTGGGAAGTTTGAGTTG	CCACCCACCAACCCAACTAACA		70	30	142

[a] Nucleotide sequences for *B2M* primers and probe were previously reported by Ogawa et al. [29].

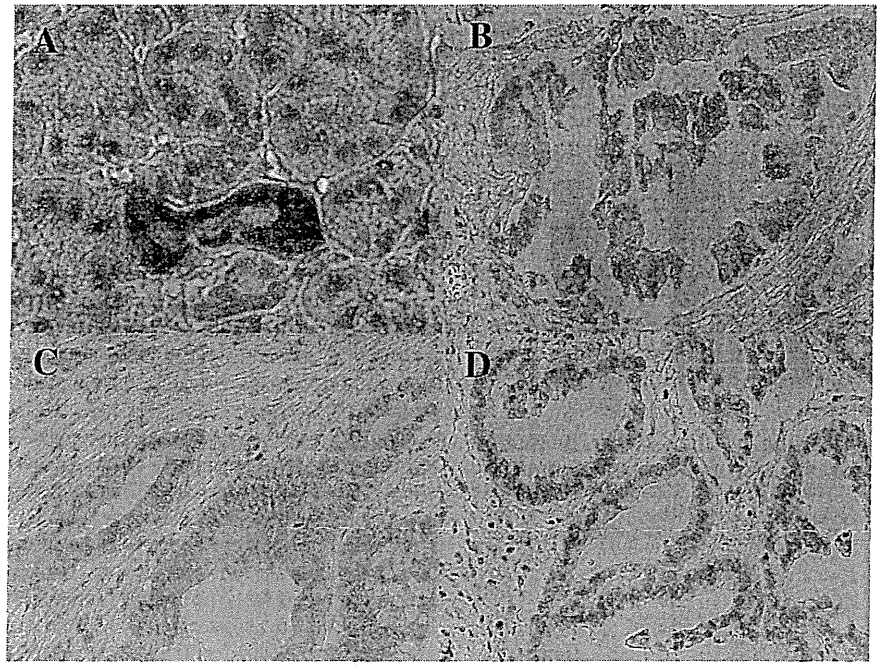

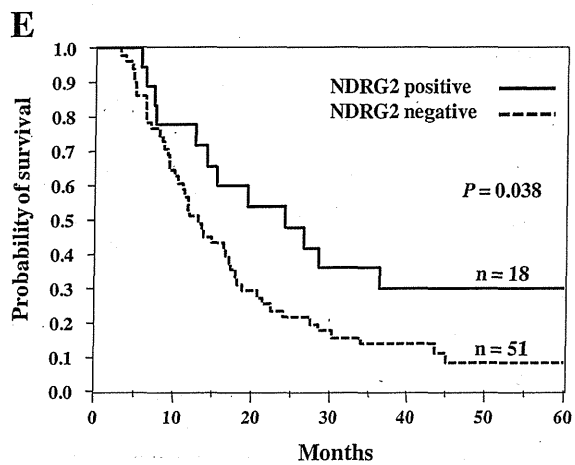

Fig. 1. (A)–(D) Results of representative immmunohistochemical analyses of NDRG2. (A) Strong immunoreactivity was observed in the cytoplasm and plasma membranes of non-neoplastic pancreatic duct (×400 magnification), and pancreatic ductal adenocarcinoma with moderate (B), weak (C), and negative (D) staining (×200 magnification). (**E**) Results of the Kaplan–Meier method indicate a poor overall survival rate of pancreatic cancer patients with negative NDRG2 expression ($P = 0.038$). Solid and dotted lines denote prognoses of NDRG2-positive and -negative patients, respectively.

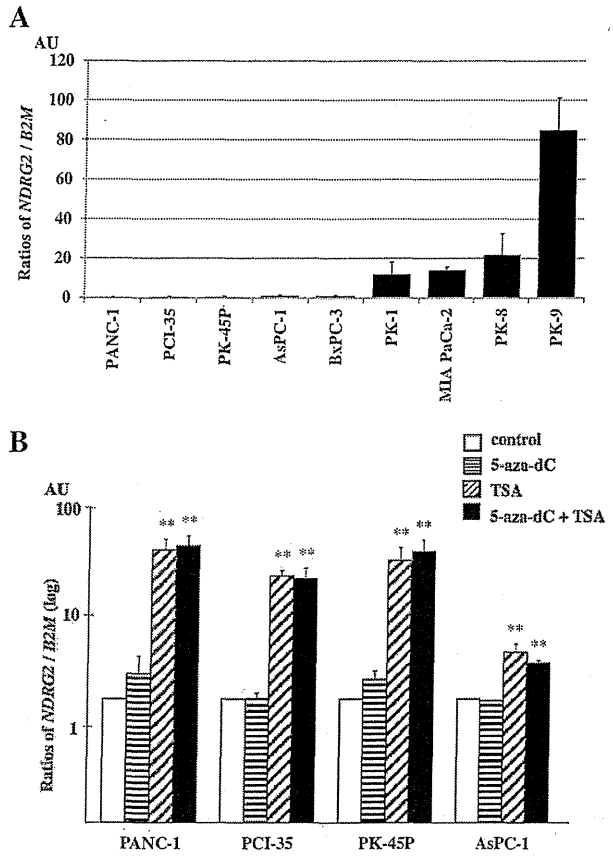

Fig. 2. Expression of *NDRG2* in human pancreatic cancer cell lines by qRT-PCR. Triplicate experiments were done, and the relative expression levels were normalized by the control *B2M* expression (arbitrary units, AU). (A) Results of 9 pancreatic cancer cells are shown. (B) Results of the four low-expressing cells are shown after 5-aza-dC and/or TSA treatments. TSA treatment up-regulated *NDRG2* expression. $^{**}P < 0.01$.

quently, cells were treated with 1 μM 5-aza-dC or 1 μM TSA (Wako, Osaka, Japan) for another 24 h. In TSA only treatment, 2×10^6 cells were plated in a 100 mm dish, and 1 μM TSA was added and cultured for 24 h. All these cells were harvested for qRT-PCR analysis.

2.7. Methylation specific PCR (MSP)

Each aliquot of 2 μg genomic DNA was modified with sodium bisulfite using an Epitect Bisulfite Kit (Qiagen) according to the manufacturer's instructions. The nucleotide sequences of primers for MSP are shown in Table 2. MSP analyses were done by methods described previously [31], and the PCR products were analyzed on 3% agarose gels. Clone A (low *NDRG2* expressing cell line) and LS174T (high *NDRG2* expressing cell line) were used as methylated and unmethylated control cells, respectively.

2.8. Statistical analysis

The Chi-square test was used to examine the correlation between *NDRG2* expression and clinicopathological factors. Survival curves were plotted using the Kaplan–Meier product-limit method, and differences between survival curves were tested using the log-rank test. The gene expression levels before and after 5-aza-dC and/or TSA treatments were analyzed by *t*-test. These statistical analyses were calculated using JMP v9.0 software (SAS Institute Inc., Cary, NC), and results were considered statistically significant when $P < 0.05$.

3. Results

3.1. NDRG2 negative staining correlated with poor prognosis in primary pancreatic cancer

We investigated the expression level of NDRG2 in surgically resected paired cancerous and corresponding normal tissues by immunohistochemical examination. Typical examples are shown in Fig. 1A–D. The spatial distribution of NDRG2 was mainly confined to the cytoplasm and plasma membrane with moderate to strong staining in noncancerous pancreatic ductal cells (Fig. 1A). According to the immunohistochemical results, of the 69 pancreatic cancer specimens examined, one exhibited a moderate NDRG2 expression in tumor cells (Fig. 1B), 17 specimens were weak (Fig. 1C), but no tumor showed stronger NDRG2 expression than normal tissue. The remaining 51 tumors were negative, as shown in Fig. 1D. One moderate and 17 weakly staining tumors were categorized as positive NDRG2 staining (18/69, 26.1%), and 51 tumors (73.9%) were negative. No significant associations were observed in clinicopathological features between positive and negative staining groups (see Table 1). However, the Kaplan–Meier analysis indicated a significant association ($P = 0.038$) between poor prognosis and negative NDRG2 expression in pancreatic cancer patients (Fig. 1E).

3.2. Restoration of NDRG2 expression after 5-aza-dC and/or TSA treatment

To determine whether epigenetic silencing contributes to suppression of the *NDRG2* transcription, we analyzed *in vitro* studies using pancreatic cancer cell lines. The mRNA expressions of *NDRG2* in 9 pancreatic cancer cell lines were determined by

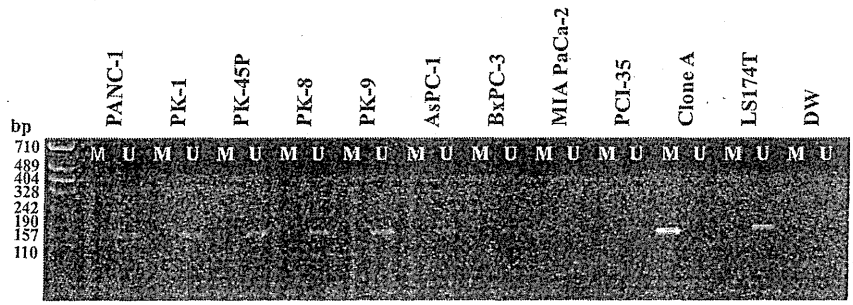

Fig. 3. MSP analyses in pancreatic cancer cell lines. Results of methylation- and unmethylation-specific PCR are indicated by M and U, respectively. All of the cell lines showed unmethylation with one exception: MIA PaCa-2 was partially methylated.

qRT-PCR analyses and found that different cell lines showed different levels of *NDRG2* expression (Fig. 2A). PANC-1, PCI-35, PK45P, AsPC-1 and BxPC-3 showed strong repression, and relatively high expression was observed in PK-9. Results of Western blot analyses correlated well with those of qRT-PCR (data not shown). We selected four pancreatic cancer cell lines (PANC-1, PCI-35, PK45P and AsPC-1) with strong repression of NDRG2 for further analyses. These cells were treated with a demethylating agent, 5-aza-dC, and/or a histone deacetylase (HDAC) inhibitor, TSA; results are shown in Fig 2B. Although no increased *NDRG2* expression was observed after the 5-aza-dC treatment alone, TSA treatment significantly up-regulated *NDRG2* expression. These results suggest that histone modification is one of the main causes for the decreased *NDRG2* expression.

3.3. Promoter hypermethylation was not involved in the decreased NDRG2 expression

It has been reported that hypermethylation is one of the main cause of suppressed expression of *NDRG2* in glioblastoma [7], meningioma [8], hepatocellular carcinoma [9], colorectal cancer [13] and oral squamous-cell carcinoma [16]. We also analyzed other types of cancer cell lines using bisulfite modified sequencing analyses and found that colon cancer cell lines Clone A and LS174T showed methylated and unmethylated CpG islands, respectively (data not shown). Using these cell lines as controls, we studied the methylation status in pancreatic cancer. All the pancreatic cancer cell lines were unmethylated except for MIA PaCa-2, which was partially methylated (Fig. 3). We further analyzed MSP using paired resected normal and cancerous pancreatic tissues from 22 pancreatic cancer patients. As expected, all of the specimens showed the unmethylated pattern, although one was partially methylated (data not shown). These results suggest that the transcriptional repression of *NDRG2* does not mainly depend on hypermethylation.

4. Discussion

Pancreatic cancer is a highly malignant gastrointestinal tumor. Only surgery with adjuvant chemotherapy can achieve a long-term perspective in patients with localized tumors. However, even under optimal treatment conditions, the 5-year survival rate do not exceed 25% [32]. To improve that situation, investigation of new therapeutic agents for pancreatic cancer treatment is essential.

Recently, an accumulation of evidence has indicated that the *NDRG2* gene downregulated in various cancers. In pancreatic cancer, however, little evidence has been reported [10], and no study on an association with prognosis has been reported to date. We demonstrated that NDRG2 expression was significantly reduced and found a significant association between poor prognosis and suppressed expression in pancreatic cancer. As there were no differences, including chemotherapeutic status, between the NDRG2 positive and negative groups, the expression of NDRG2 is likely to be an independent prognostic factor in pancreatic cancer.

We found that histone modification is one of the main mechanisms for downregulating the *NDRG2* expression in pancreatic cancer, and no such mechanisms have previously been reported to control *NDRG2* expression. Histone modification has emerged as a critical component of an epigenetic indexing system demarcating transcriptionally active chromatin domains. In general, while increased histone acetylation is associated with open and active chromatin and increased transcription, deacetylated histones are associated with condensed chromatin and transcriptional repression [33]. Histone deacethylases (HDACs) remove acethyl groups from histones, thereby inducing chromatin condensation and transcriptional repression [34]. Eighteen HDACs have been identified in humans, and they are subdivided into four classes based on their homology to yeast HDACs, their subcellular localization and their enzymatic activities [35]. In pancreatic cancer, high HDAC I expression together with HIF1α were associated with poor prognosis in a series of 39 pancreatic carcinomas [36]. Class I- and class II-selective HDAC inhibitors both synergize in inducing growth arrest and death of pancreatic cells [37]. Other research has also increased our understanding of HDAC function in pancreatic cancer [38]. At least 12 different HDAC inhibitors are undergoing clinical trials as monotherapies or in combination with other adjuvant therapies such as retinoic acid, paclitaxel, gemcitabine, or radiation in patients with various hematologic and solid tumors of the lung, breast, kidney, or bladder as well as with melanoma, glioblastoma, leukemia, lymphomas, and multiple myeloma [39,40]. In pancreatic cancer, promising results have been shown using suberoylanilindehydroxamic acid (SAHA), butyrate, and some other HDAC inhibitors in experimental studies [38,41]. TSA induced G2 arrest and apoptosis in human pancreatic cancer cell lines with mutated TP53 by induction of CDKN1A [42]. Synergistic enhancement of the cytotoxicity of TSA with proteasome inhibitor has also been reported [43]. Our present results that *NDRG2* expression is suppressed mainly by histone-mediated mechanisms and that suppression of *NDRG2* correlates with poor prognosis may provide some valuable clues for the clinical management of patients with pancreatic cancer utilizing a HDAC inhibitor.

The present study indicates that *NDRG2* is likely to be a tumor suppressor gene, reinforcing the data previously reported. In addition, we have demonstrated that inactivation of *NDRG2* associates with poor prognosis in pancreatic cancer. Furthermore, we conclude that epigenetic silencing, such as histone modification, might be the major cause of the frequent loss of NDRG2 expression. Further studies elucidating NDRG2 function will provide a unique and powerful tool for developing novel and useful applications for diagnosis and treatment of patients with pancreatic cancer.

Acknowledgments

We are grateful to Dr. Barbara Lee Smith Pierce (University of Maryland University College) for editorial work in the preparation of this manuscript, to Naomi Kanai, Emiko Kondo, Emiko Shibuya, Midori Chiba, and Keiko Inabe for excellent technical assistance, and to Biomedical Research Core (Tohoku University School of Medicine) for technical support. This work was supported in part by Grants-in-Aid (Grant #17015003, 22591512, and 23590452) and by the Academic Frontier Project for Private Universities: matching fund subsidy 2006–2010 from the Ministry of Education, Culture, Sports, Science and Technology of Japan, a Grant-in-Aid for Cancer Research (Grant #18–19) from the Ministry of Health, Labour and Welfare of Japan, Pancreas Research Foundation of Japan, and Gonryo Medical Foundation.

References

[1] R. Siegel, D. Naishadham, A. Jemal, Cancer statistics, CA Cancer J. Clin. 62 (2012) (2012) 10–29.

[2] M. Ducreux, V. Boige, D. Goere, E. Deutsch, P. Ezra, D. Elias, D. Malka, The multidisciplinary management of gastrointestinal cancer. Pancreatic cancer: from pathogenesis to cure, Best Pract. Res. Clin. Gastroenterol. 21 (2007) 997–1014.

[3] S. Boulkroun, M. Fay, M.C. Zennaro, B. Escoubet, F. Jaisser, M. Blot-Chabaud, N. Farman, N. Courtois-Coutry, Characterization of rat NDRG2 (N-Myc downstream regulated gene 2), a novel early mineralocorticoid-specific induced gene, J. Biol. Chem. 277 (2002) 31506–31515.

[4] Y. Deng, L. Yao, L. Chau, S.S. Ng, Y. Peng, X. Liu, W.S. Au, J. Wang, F. Li, S. Ji, H. Han, X. Nie, Q. Li, H.F. Kung, S.Y. Leung, M.C. Lin, N-Myc downstream-regulated gene 2 (NDRG2) inhibits glioblastoma cell proliferation, Int. J. Cancer 106 (2003) 342–347.

[5] X. Qu, Y. Zhai, H. Wei, C. Zhang, G. Xing, Y. Yu, F. He, Characterization and expression of three novel differentiation-related genes belong to the human NDRG gene family, Mol. Cell. Biochem. 229 (2002) 35–44.
[6] V. Melotte, X. Qu, M. Ongenaert, W. van Criekinge, A.P. de Bruine, H.S. Baldwin, M. van Engeland, The N-myc downstream regulated gene (NDRG) family: Diverse functions, multiple applications, FASEB J. 24 (2010) 4153–4166.
[7] M. Tepel, P. Roerig, M. Wolter, D.H. Gutmann, A. Perry, G. Reifenberger, M.J. Riemenschneider, Frequent promoter hypermethylation and transcriptional downregulation of the NDRG2 gene at 14q11.2 in primary glioblastoma, Int. J. Cancer 123 (2008) 2080–2086.
[8] E.A. Lusis, M.A. Watson, M.R. Chicoine, M. Lyman, P. Roerig, G. Reifenberger, D.H. Gutmann, A. Perry, Integrative genomic analysis identifies NDRG2 as a candidate tumor suppressor gene frequently inactivated in clinically aggressive meningioma, Cancer Res. 65 (2005) 7121–7126.
[9] D.C. Lee, Y.K. Kang, W.H. Kim, Y.J. Jang, D.J. Kim, I.Y. Park, B.H. Sohn, H.A. Sohn, H.G. Lee, J.S. Lim, J.W. Kim, E.Y. Song, D.M. Kim, M.N. Lee, G.T. Oh, S.J. Kim, K.C. Park, H.S. Yoo, J.Y. Choi, Y.I. Yeom, Functional and clinical evidence for NDRG2 as a candidate suppressor of liver cancer metastasis, Cancer Res. 68 (2008) 4210–4220.
[10] X.L. Hu, X.P. Liu, S.X. Lin, Y.C. Deng, N. Liu, X. Li, L.B. Yao, NDRG2 expression and mutation in human liver and pancreatic cancers, World J. Gastroenterol. 10 (2004) 3518–3521.
[11] H. Shi, N. Li, S. Li, C. Chen, W. Wang, C. Xu, J. Zhang, H. Jin, H. Zhang, H. Zhao, W. Song, Q. Feng, X. Feng, X. Shen, L. Yao, Q. Zhao, Expression of NDRG2 in esophageal squamous cell carcinoma, Cancer Sci. 101 (2010) 1292–1299.
[12] S.C. Choi, S.R. Yoon, Y.P. Park, E.Y. Song, J.W. Kim, W.H. Kim, Y. Yang, J.S. Lim, H.G. Lee, Expression of NDRG2 is related to tumor progression and survival of gastric cancer patients through Fas-mediated cell death, Exp. Mol. Med. 39 (2007) 705–714.
[13] A. Piepoli, R. Cotugno, G. Merla, A. Gentile, B. Augello, M. Quitadamo, A. Merla, A. Panza, M. Carella, R. Maglietta, A. D'Addabbo, N. Ancona, S. Fusilli, F. Perri, A. Andriulli, Promoter methylation correlates with reduced NDRG2 expression in advanced colon tumour, BMC Med. Genomics 2 (2009) 11.
[14] H. Shi, H. Jin, D. Chu, W. Wang, J. Zhang, C. Chen, C. Xu, D. Fan, L. Yao, Suppression of N-myc downstream-regulated gene 2 is associated with induction of Myc in colorectal cancer and correlates closely with differentiation, Biol. Pharm. Bull. 32 (2009) 968–975.
[15] H. Zhao, J. Zhang, J. Lu, X. He, C. Chen, X. Li, L. Gong, G. Bao, Q. Fu, S. Chen, W. Lin, H. Shi, J. Ma, X. Liu, Q. Ma, L. Yao, Reduced expression of N-Myc downstream-regulated gene 2 in human thyroid cancer, BMC Cancer 8 (2008) 303.
[16] H. Furuta, Y. Kondo, S. Nakahata, M. Hamasaki, S. Sakoda, K. Morishita, NDRG2 is a candidate tumor-suppressor for oral squamous-cell carcinoma, Biochem. Biophys. Res. Commun. 391 (2010) 1785–1791.
[17] L. Gao, G.J. Wu, X.W. Liu, R. Zhang, L. Yu, G. Zhang, F. Liu, C.G. Yu, J.L. Yuan, H. Wang, L.B. Yao, Suppression of invasion and metastasis of prostate cancer cells by overexpression of NDRG2 gene, Cancer Lett. 310 (2011) 94–100.
[18] S.P. Song, S.B. Zhang, R. Liu, L. Yao, Y.Q. Hao, M.M. Liao, Y.D. Zhang, Z.H. Li, NDRG2 down-regulation and CD24 up-regulation promote tumor aggravation and poor survival in patients with gallbladder carcinoma, Med. Oncol. 29 (2012) 1879–1885.
[19] M.P. Tschan, D. Shan, J. Laedrach, M. Eyholzer, E.O. Leibundgut, G.M. Baerlocher, A. Tobler, D. Stroka, M.F. Fey, NDRG1/2 expression is inhibited in primary acute myeloid leukemia, Leuk. Res. 34 (2010) 393–398.
[20] S.J. Li, W.Y. Wang, B. Li, B. Chen, B. Zhang, X. Wang, C.S. Chen, Q.C. Zhao, H. Shi, L. Yao, Expression of NDRG2 in human lung cancer and its correlation with prognosis, Med. Oncol. 30 (2013) 421.
[21] N. Liu, L. Wang, X. Li, Q. Yang, X. Liu, J. Zhang, Y. Wu, S. Ji, Y. Zhang, A. Yang, H. Han, L. Yao, N-Myc downstream-regulated gene 2 is involved in p53-mediated apoptosis, Nucleic Acids Res. 36 (2008) 5335–5349.
[22] A. Kim, M.J. Kim, Y. Yang, J.W. Kim, Y.I. Yeom, J.S. Lim, Suppression of NF-kappaB activity by NDRG2 expression attenuates the invasive potential of highly malignant tumor cells, Carcinogenesis 30 (2009) 927–936.
[23] N. Liu, L. Wang, X. Liu, Q. Yang, J. Zhang, W. Zhang, Y. Wu, L. Shen, Y. Zhang, A. Yang, H. Han, L. Yao, Promoter methylation, mutation, and genomic deletion are involved in the decreased NDRG2 expression levels in several cancer cell lines, Biochem. Biophys. Res. Commun. 358 (2007) 164–169.
[24] J. Zhang, F. Li, X. Liu, L. Shen, J. Liu, J. Su, W. Zhang, Y. Deng, L. Wang, N. Liu, W. Han, S. Ji, A. Yang, H. Han, L. Yao, The repression of human differentiation-related gene NDRG2 expression by Myc via Miz-1-dependent interaction with the NDRG2 core promoter, J. Biol. Chem. 281 (2006) 39159–39168.
[25] International Union Against Cancer (UICC), TNM Classification of Malignant Tumor, sixth ed., Wiley-Liss, New York, 2002.
[26] T. Furukawa, M. Sunamura, F. Motoi, S. Matsuno, A. Horii, Potential tumor suppressive pathway involving DUSP6/MKP-3 in pancreatic cancer, Am. J. Pathol. 162 (2003) 1807–1815.
[27] H. Sasaki, K. Miura, A. Horii, N. Kaneko, W. Fujibuchi, L. Kiseleva, Z. Gu, Y. Murata, H. Karasawa, T. Mizoi, T. Kobayashi, M. Kinouchi, S. Ohnuma, N. Yazaki, M. Unno, I. Sasaki, Orthotopic implantation mouse model and cDNA microarray analysis indicates several genes potentially involved in lymph node metastasis of colorectal cancer, Cancer Sci. 99 (2008) 711–719.
[28] T. Tabata, N. Tsukamoto, A.A. Fooladi, S. Yamanaka, T. Furukawa, M. Ishida, D. Sato, Z. Gu, H. Nagase, S. Egawa, M. Sunamura, A. Horii, RNA interference targeting against S100A4 suppresses cell growth and motility and induces apoptosis in human pancreatic cancer cells, Biochem. Biophys. Res. Commun. 390 (2009) 475–480.
[29] K. Ogawa, K. Shiga, S. Saijo, T. Ogawa, N. Kimura, A. Horii, A novel G106D alteration of the SDHD gene in a pedigree with familial paraganglioma, Am. J. Med. Genet. A. 140 (2006) 2441–2446.
[30] N. Kaneko, K. Miura, Z. Gu, H. Karasawa, S. Ohnuma, H. Sasaki, N. Tsukamoto, S. Yokoyama, A. Yamamura, H. Nagase, C. Shibata, I. Sasaki, A. Horii, SiRNA-mediated knockdown against CDCA1 and KNTC2, both frequently overexpressed in colorectal and gastric cancers, suppresses cell proliferation and induces apoptosis, Biochem. Biophys. Res. Commun. 390 (2009) 1235–1240.
[31] M. Sato, Y. Mori, A. Sakurada, S. Fujimura, A. Horii, The H-cadherin (CDH13) gene is inactivated in human lung cancer, Hum. Genet. 103 (1998) 96–101.
[32] J.P. Neoptolemos, D.D. Stocken, C. Bassi, P. Ghaneh, D. Cunningham, D. Goldstein, R. Padbury, M.J. Moore, S. Gallinger, C. Mariette, M.N. Wente, J.R. Izbicki, H. Friess, M.M. Lerch, C. Dervenis, A. Olah, G. Butturini, R. Doi, P.A. Lind, D. Smith, J.W. Valle, D.H. Palmer, J.A. Buckels, J. Thompson, C.J. McKay, C.L. Rawcliffe, M.W. Buchler, European study group for pancreatic, ADJUVANT chemotherapy with fluorouracil plus folinic acid vs gemcitabine following pancreatic cancer resection: a randomized controlled trial, JAMA 304 (2010) 1073–1081.
[33] K.N. Bhalla, Epigenetic and chromatin modifiers as targeted therapy of hematologic malignancies, J. Clin. Oncol. 23 (2005) 3971–3993.
[34] M. Haberland, R.L. Montgomery, E.N. Olson, The many roles of histone deacetylases in development and physiology: implications for disease and therapy, Nat. Rev. Genet. 10 (2009) 32–42.
[35] S. Thiagalingam, K.H. Cheng, H.J. Lee, N. Mineva, A. Thiagalingam, J.F. Ponte, Histone deacetylases: unique players in shaping the epigenetic histone code, Ann. N.Y. Acad. Sci. 983 (2003) 84–100.
[36] K. Miyake, T. Yoshizumi, S. Imura, K. Sugimoto, E. Batmunkh, H. Kanemura, Y. Morine, M. Shimada, Expression of hypoxia-inducible factor-1alpha, histone deacetylase 1, and metastasis-associated protein 1 in pancreatic carcinoma: correlation with poor prognosis with possible regulation, Pancreas 36 (2008) e1–e9.
[37] G. Wang, J. He, J. Zhao, W. Yun, C. Xie, J.W. Taub, A. Azmi, R.M. Mohammad, Y. Dong, W. Kong, Y. Guo, Y. Ge, Class I and Class II histone deacetylases are potential therapeutic targets for treating pancreatic cancer, PLoS ONE 7 (2012) e52095.
[38] G. Schneider, O.H. Kramer, P. Fritsche, S. Schuler, R.M. Schmid, D. Saur, Targeting histone deacetylases in pancreatic ductal adenocarcinoma, J. Cell Mol. Med. 14 (2010) 1255–1263.
[39] M. Dokmanovic, C. Clarke, P.A. Marks, Histone deacetylase inhibitors: overview and perspectives, Mol. Cancer Res. 5 (2007) 981–989.
[40] M. New, H. Olzscha, N.B. La Thangue, HDAC inhibitor-based therapies: can we interpret the code?, Mol Oncol. 6 (2012) 637–656.
[41] D.I. Dovzhanskiy, S.M. Arnold, T. Hackert, I. Oehme, O. Witt, K. Felix, N. Giese, J. Werner, Experimental in vivo and in vitro treatment with a new histone deacetylase inhibitor belinostat inhibits the growth of pancreatic cancer, BMC Cancer 12 (2012) 226.
[42] M. Donadelli, C. Costanzo, L. Faggioli, M.T. Scupoli, P.S. Moore, C. Bassi, A. Scarpa, M. Palmieri, Trichostatin A, an inhibitor of histone deacetylases, strongly suppresses growth of pancreatic adenocarcinoma cells, Mol. Carcinog. 38 (2003) 59–69.
[43] J. Bai, A. Demirjian, J. Sui, W. Marasco, M.P. Callery, Histone deacetylase inhibitor trichostatin A and proteasome inhibitor PS-341 synergistically induce apoptosis in pancreatic cancer cells, Biochem. Biophys. Res. Commun. 348 (2006) 1245–1253.

Cancer Science
The official journal of the Japanese Cancer Association

Overexpression of the DNA sensor proteins, absent in melanoma 2 and interferon-inducible 16, contributes to tumorigenesis of oral squamous cell carcinoma with p53 inactivation

Yuudai Kondo,[1,2] Kentaro Nagai,[1,2] Shingo Nakahata,[2] Yusuke Saito,[2] Tomonaga Ichikawa,[2] Akira Suekane,[2] Tomohiko Taki,[3] Reika Iwakawa,[4] Masato Enari,[5] Masafumi Taniwaki,[3] Jun Yokota,[4] Sumio Sakoda[1] and Kazuhiro Morishita[2,6]

[1]Division of Oral and Maxillofacial Surgery, Medicine of Sensory and Motor Organs, and [2]Division of Tumor and Cellular Biochemistry, Department of Medical Sciences, Faculty of Medicine, University of Miyazaki, Miyazaki; [3]Department of Hematology and Oncology, Kyoto Prefectural University of Medicine, Kyoto; [4]Division of Multistep Carcinogenesis, and [5]Division of Refractory Cancer, National Cancer Center Research Institute, Tokyo, Japan

(Received September 1, 2011/Revised December 27, 2011/Accepted December 29, 2011/Accepted manuscript online February 9, 2012/Article first published online February 23, 2012)

The development of oral squamous cell carcinoma (OSCC) is a multistep process that requires the accumulation of genetic alterations. To identify genes responsible for OSCC development, we performed high-density single nucleotide polymorphism array analysis and genome-wide gene expression profiling on OSCC tumors. These analyses indicated that the absent in melanoma 2 (*AIM2*) gene and the interferon-inducible gene 16 (*IFI16*) mapped to the hematopoietic interferon-inducible nuclear proteins. The 200-amino-acid repeat gene cluster in the amplified region of chromosome 1q23 is overexpressed in OSCC. Both AIM2 and IFI16 are cytoplasmic double-stranded DNA sensors for innate immunity and act as tumor suppressors in several human cancers. Knockdown of AIM2 or IFI16 in OSCC cells results in the suppression of cell growth and apoptosis, accompanied by the downregulation of nuclear factor kappa-light-chain-enhancer of activated B cells activation. Because all OSCC cell lines have reduced p53 activity, wild-type p53 was introduced in p53-deficient OSCC cells. The expression of wild-type p53 suppressed cell growth and induced apoptosis via suppression of nuclear factor kappa-light-chain-enhancer of activated B cells activity. Finally, the co-expression of AIM2 and IFI16 significantly enhanced cell growth in p53-deficient cells; in contrast, the expression of AIM2 and/or IFI16 in cells bearing wild-type p53 suppressed cell growth. Moreover, AIM2 and IFI16 synergistically enhanced nuclear factor kappa-light-chain-enhancer of activated B cells signaling in p53-deficient cells. Thus, expression of AIM2 and IFI16 may have oncogenic activities in the OSCC cells that have inactivated the p53 system. (*Cancer Sci* 2012; 103: 782–790)

Oral squamous cell carcinoma is commonly found in low-income communities. This cancer mainly affects older men; 90% of cases are in men over 45 years old who have been exposed to risk factors including tobacco and/or alcohol (International Agency for Research on Cancer [IARC] 2004). OSCC is the sixth most common cancer worldwide and affects approximately 270 000 people each year.[1] The incidence and rate of mortality from OSCC are rising in several regions of Europe, Australia and Asia, including Japan. Despite recent progress in OSCC diagnosis and therapy, the 5-year survival rate has not improved in more than two decades.[2]

Oral carcinogenesis is a multifactorial cascade involving numerous genetic changes that affect the activity of oncogenes, tumor suppressor genes and other classes of disease-related genes. Chronic exposure to carcinogens, such as tobacco, causes genetic changes in the epithelial cells of the oral mucosa. The activation of the *COX-2*,[3] epidermal growth factor receptor,[4] and cyclin D1 oncogenes and the inactivation of the *p16* and *p53* tumor suppressor genes have also been reported in OSCC.[5–7] In addition to tobacco smoke exposure, chronic alcohol use and chronic inflammation can both induce genetic alterations.[3] The causative agent of cervical cancer, HPV is also reportedly associated with head and neck cancers, including OSCC.[8] Compared to HPV-negative cases, HPV-positive OSCC have an intact *p16* gene and wild-type *p53*, and harbor frequent genetic alterations of the *p16* and *p53* genes.[9,10] The HPV oncoproteins E6 and E7 exploit the ubiquitin-proteasome system to degrade and functionally inactivate negative cell-regulatory proteins, including members of the p110 (Rb) family and p53; this process may primarily contribute to HPV-induced carcinogenesis.[11]

The innate immune system provides nonspecific protection and enhances the adaptive immune response against a variety of pathogens, including HPV. The IFI16 and AIM2 proteins were recently found to be innate immune sensors for cytosolic dsDNA. Upon sensing dsDNA, the IFI16 protein induces the expression of IFN-β,[12] whereas the AIM2 protein forms an inflammasome that promotes the secretion of interleukin-1β.[13] Both *IFI16* and *AIM2* belong to the HIN-200 gene family found on human and mouse chromosome 1; they are positively regulated by type I and II INF and have been described as regulators of cell proliferation, differentiation, apoptotic and inflammatory processes.[14] The overexpression of IFI16 in cells inhibits cell proliferation by potentiating the p53/p21- and Rb/E2F-mediated inhibition of cell-cycle progression, and IFI16 downregulation contributes to oncogenesis.[15,16] Also, AIM2 expression suppresses cell proliferation and tumorigenicity of human breast cancer cells.[17] Therefore, it has been proposed that *AIM2* and *IFI16* function as tumor suppressor genes.

To identify genes involved in OSCC tumorigenesis, OSCC tumors were submitted to genomic analysis by high-density SNP array analysis. A number of amplified or deleted genomic regions in OSCC cells were identified, and a series of genes in the genetically altered regions were selected by expression

[6]To whom correspondence should be addressed.
E-mail: kmorishi@med.miyazaki-u.ac.jp

doi: 10.1111/j.1349-7006.2012.02211.x

profile analysis. Of these genes, the NIH-200 gene family locus on chromosome 1q23 was frequently amplified, and *AIM2* and *IFI16* in the NIH-200 gene family were highly expressed in most OSCC tumors. Although *AIM2* and *IFI16* were reported to be tumor suppressors, the expression of AIM2 and IFI16 enhanced the cell growth of OSCC cell lines. Here we describe a mechanism by which *AIM2* and *IFI16* may be functioning as oncogenes in OSCC.

Materials and Methods

Materials and Methods are given in Data S1 and Data S2 in the supporting information.

Results

Higher expression of AIM2 and IFI16 with frequent amplification at 1q23 in OSCC. To identify novel genes responsible for tumorigenesis in OSCC, we performed high-density SNP array analysis on 28 OSCC tumor samples using an Affymetrix Human Mapping 250K Sty Array (Affymetrix, Santa Clara, CA, USA). The most frequent gains involved segments of chromosomes 1, 3q, 5p, 6p, 7p, 8q, 9q, 14, 15, 16, 17, 19, 20 and 22, whereas the most frequent losses involved segments of chromosomes 3p, 4, 5q, 8p, 10p, 18q and 21q (Fig. S1). Of these, 77 were amplified and ranged in size from 0.3 to 49.3 Mb, and four were found to be deleted and ranged in size from 0.2 to 0.6 Mb, in more than 14 of 28 OSCC tumor samples (Table S1).

To select candidate genes within the regions with altered copy numbers, we analyzed a data set from the NCBI Gene Expression Omnibus (http://www.ncbi.nlm.nih.gov/geo/), which contained the gene expression data of four oral tissue samples from healthy volunteers and 16 tumor samples from OSCC patients.[18] Of the genes in the amplified regions, 27 were expressed at more than two-fold higher levels ($P < 0.01$) (Table S1-1). However, no genes that were downregulated more than two-fold were identified in the deleted region (Table S1 2). Interestingly, 15 of the 27 candidates were previously reported to be cancer-related genes. The genes linked to OSCC included keratin 19, lectin, galactoside-binding, soluble, 1 and *IFI16*.[19–21] Furthermore, five of the 27 upregulated genes were also found to be *IFI* genes, including *IFI6*, *IFI35*, *AIM2*, *IFI16* and bone marrow stromal cell antigen-2. Among them, the *AIM2* and *IFI16* genes are located within the HIN-200 gene cluster on 1q23 and have been identified as a new family of innate immune DNA sensors for intracellular DNA called AIM2-like receptors.[12] Because chronic inflammation and infection contribute to the development of several types of cancer, we analyzed the HIN-200 gene cluster locus on 1q23.

Based on the SNP array analysis from 28 OSCC cases, four members of the HIN-200 family, along with other 19 genes, were located in the 1.3-Mb common region of amplification at 1q23 (Fig. 1a). The expression profiles showed that IFI16 and AIM2 are highly expressed in OSCC, but no significant differences in the expression levels of the other 21 genes, including myeloid cell nuclear differentiation antigen (*MNDA*) and pyrin and HIN domain family, member 1 (*PYHIN*), were observed between the OSCC and control oral tissues (Fig. S2a–c). Using semi-quantitative and quantitative real-time PCR, we confirmed statistically significant higher expression of AIM2 and IFI16 in tumor samples from OSCC patients and OSCC cell lines ($P < 0.05$) (Figs 1b–e, S2d). Moreover, the expression of AIM2 was significantly higher in the group with metastasis (N1) than in that without metastasis (N0) ($P < 0.05$). To confirm the relationship between genomic amplification and mRNA expression levels of *AIM2* and *IFI16*, a scatter plot was used to evaluate the correlation between the two variables in 20 OSCC tumor samples and eight cell lines. As shown in Figure 1(f), we found weak but positive correlations between the DNA copy numbers and mRNA expression levels for the two genes. Although a few cases did not show gene amplification or overexpression of the *AIM2* and *IFI16* genes, the majority of cases presented gene amplification and high expression of these two genes. Thus, in the HIN-200 family of genes, *AIM2* and *IFI16*, are overexpressed in OSCC, and this overexpression is frequently accompanied by gene amplification.

High expression of AIM2 and IFI16 enhanced cell growth by preventing apoptosis in OSCC cells. An important inflammasome component, AIM2 senses potentially dangerous cytoplasmic DNA and regulates caspase-1 activation.[13] Cytoplasmic overexpression of AIM2 also reportedly reduces cell proliferation and increases susceptibility to cell death in transfected murine fibroblasts. To determine whether the high expression levels of AIM2 or IFI16 have an effect on OSCC cell growth, we introduced an shRNA expression vector against AIM2 (shAIM2), IFI16 (shIFI16) or luciferase (shLuc) as a control into the human OSCC cell line SAS. SAS cells expressing the shRNA for either AIM2 (SAS/shAIM2) or IFI16 (SAS/shIFI16) had decreased growth rates relative to control-transfected cells (SAS/shLuc) (Fig. 2a,b). Notably, downregulation of both AIM2 and IFI16 expression had the most significant effect on growth inhibition. Similar effects were observed in the HSC4-OSCC cell line (Fig. S3). Next, apoptosis and cell cycle were investigated by flow cytometry with propidium iodide (PI) and Annexin V, respectively. The cell cycle profiles of SAS/shAIM2 and SAS/shIFI16 cells were not significantly different from those of the control SAS/shLuc cells, but the SAS/shAIM2 and SAS/shIFI16 cells exhibited a higher percentage of cell death (sub-G1 population) than the SAS/shLuc cells (Figs 2c, S4). In the SAS/shAIM2 and SAS/shIFI16 cells, the percentage of cells that bound Annexin V increased approximately 10- and 3-fold, respectively, compared with the SAS/shLuc cells (Fig. 2d). These data suggest that high expression of AIM2 and IFI16 enhances cell survival by preventing OSCC cells from entering apoptosis.

Activation of NF-κB signaling by AIM2 and IFI16 in OSCC. Once bound to the DNA in the cytoplasm, AIM2 activates both NF-κB and caspase-1,[13] and cytosolic DNA also triggers NF-κB activation by IFI16.[12] To clarify the mechanisms by which constitutive expression of AIM2 and/or IFI16 prevent apoptosis in OSCC cells, we studied caspase-1 and NF-κB for constitutive activation in OSCC. Initially, the SAS-OSCC cell lines transfected with the shLuc, shIFI16 or shAIM2 vectors were examined for the expression of cleaved caspase-1 by immunoblot analysis using a cleaved caspase-1 specific antibody. Cleaved caspase-1 was not detected in any of these cell lines but was detected in the human acute monocytic leukemia cell line (THP-1) transfected with poly deoxyadenylic-deoxythymidylic acid (poly[dA:dT]) as a positive control (Fig. S5a). The cleaved form of caspase-1 was also not detected in seven of the eight OSCC cell lines except for HSQ89 (data not shown). In addition, the treatment of SAS-OSCC cells with poly(dA:dT) had no effect on caspase-1 cleavage (Fig. S5b), suggesting that dsDNA could not trigger the formation of the AIM2 inflammasome in OSCC cells.

To assess NF-κB activation in OSCC, we measured IκBα protein in eight OSCC cell lines and 10 primary OSCC tumors by immunoblot analysis. We observed significantly higher levels of phosphorylated IκBα and lower levels of total IκBα in most OSCC cell lines and primary tumor samples compared to control gingival tissues (Fig. 3a). This result suggests that NF-κB signaling is often activated in OSCC. To confirm this hypothesis, four OSCC cell lines (HSQ89, HSC3, HSC4 and SAS) were treated with various concentrations of the NF-κB

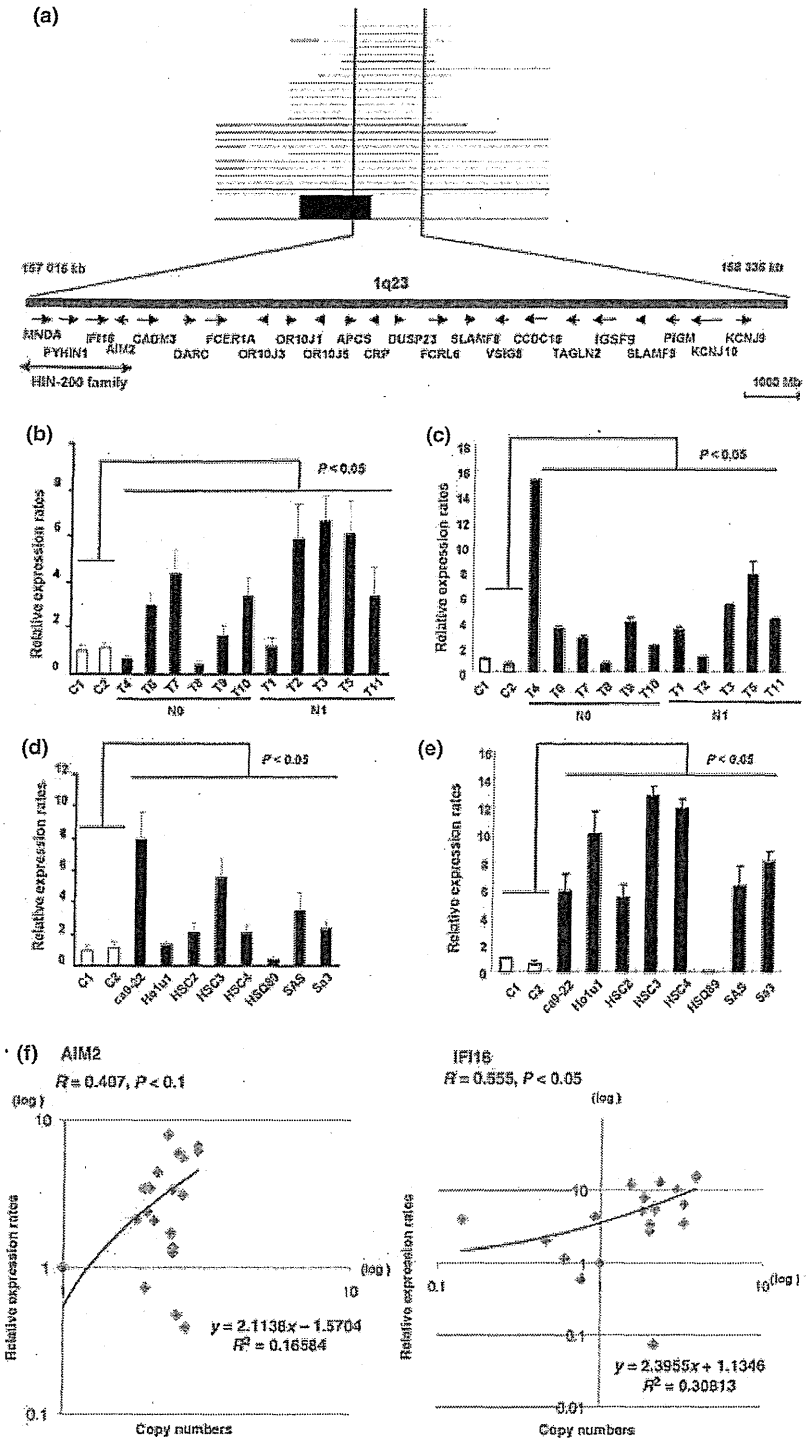

Fig. 1. Overexpression of IFI16 and AIM2 mRNA in OSCC. (a) Recurrent genetic changes are depicted based on the copy number analyzer for GeneChip (CNAG) output of the single nucleotide polymorphism array analysis of 28 oral squamous cell carcinoma (OSCC) samples, which include gains at the *IFI16* and *AIM2* loci on 1q23. Regions showing copy number gains are indicated by horizontal lines. *AIM2*, absent in melanoma 2; *APCS*, amyloid P component, serum; *CADM3*, cell adhesion molecule 3; *CCDC19*, coiled-coil domain containing 19; *CRP*, C-reactive protein, pentraxin-related; *DARC*, Duffy blood group, chemokine receptor; *DUSP23*, dual specificity phosphatase 23; *FCER1A*, Fc fragment of IgE, high affinity I, receptor for: alpha polypeptide; *FCRL6*, Fc receptor-like 6; *IFI16*, interferon, gamma-inducible protein 16; *IGSF9*, immunoglobulin superfamily, member 9; *KCNJ9*, potassium inwardly-rectifying channel, subfamily J, member 9; *KCNJ10*, potassium inwardly-rectifying channel, subfamily J, member 10; *MNDA*, myeloid cell nuclear differentiation antigen; *OR10J1*, olfactory receptor, family 10, subfamily J, member 1; *OR10J3*, olfactory receptor, family 10, subfamily J, member 3; *OR10J5*, olfactory receptor, family 10, subfamily J, member 5; *PIGM*, phosphatidylinositol glycan anchor biosynthesis, class M; *PYHIN1*, pyrin and HIN domain family, member 1; *SLAMF8*, SLAM family member 8; *SLAMF9*, SLAM family member 9; *TAGLN2*, transgelin 2; *VSIG8*, V-set and immunoglobulin domain containing 8. (b,d) Expression of the AIM2 and (c,e) IFI16 mRNA were examined in 11 primary OSCC and eight OSCC cell lines (Ca9-22, Ho1u1, HSC2, HSC3, HSC4, HSQ89, SAS and Sa3) by quantitative real-time PCR. Normal gingival tissues from normal volunteers were used as controls. (f) Scatter plot of DNA copy number versus mRNA expression for *AIM2* (left) and *IFI16* (right). Correlations were quantified using the Spearman's rank correlation coefficient. AIM2, absent in melanoma; HIN-200, Hematopoietic interferon-inducible nuclear proteins with a 200-amino-acid repeat; IFI16, interferon-inducible 16; N0, without metastasis; N1, with metastasis.

inhibitor Bay 11-7082 for 48 h and examined for cell viability. In three of the four cell lines (not HSQ89), cell viability was inhibited by Bay 11-7082 treatment, although the effect varied among the cell lines (Fig. 3b). To determine whether the observed cell death was due to apoptosis, two cell lines, SAS and HSC3, treated with or without Bay 11-7082 were stained with Annexin V/PI and analyzed by flow cytometry. Over 90% of the OSCC cell lines underwent apoptosis 48 h after treatment with 10-μM Bay11-7082 (Figs 3c, S6). Moreover, there was a dose-dependent increase in the total IκBα and decrease in the phosphorylated IκBα levels after exposure to 1–10-μM Bay11-7082 (Fig. 3d). To determine whether high expression of AIM2 and/or IFI16 contributes to the constitutive NF-κB activation in OSCC, SAS cells were transfected with either shIFI16 and/or shAIM2 vectors and analyzed for IκBα expression. As expected, the SAS cells treated with shIFI16, shAIM2 or both shRNA significantly increased protein levels of phosphorylated-IκBα and reduced the total IκBα levels compared with control cells transfected with shLuc and parental cells (Fig. 3e). The reduction of NF-κB activation by shIFI16 or

doi: 10.1111/j.1349-7006.2012.02211.x

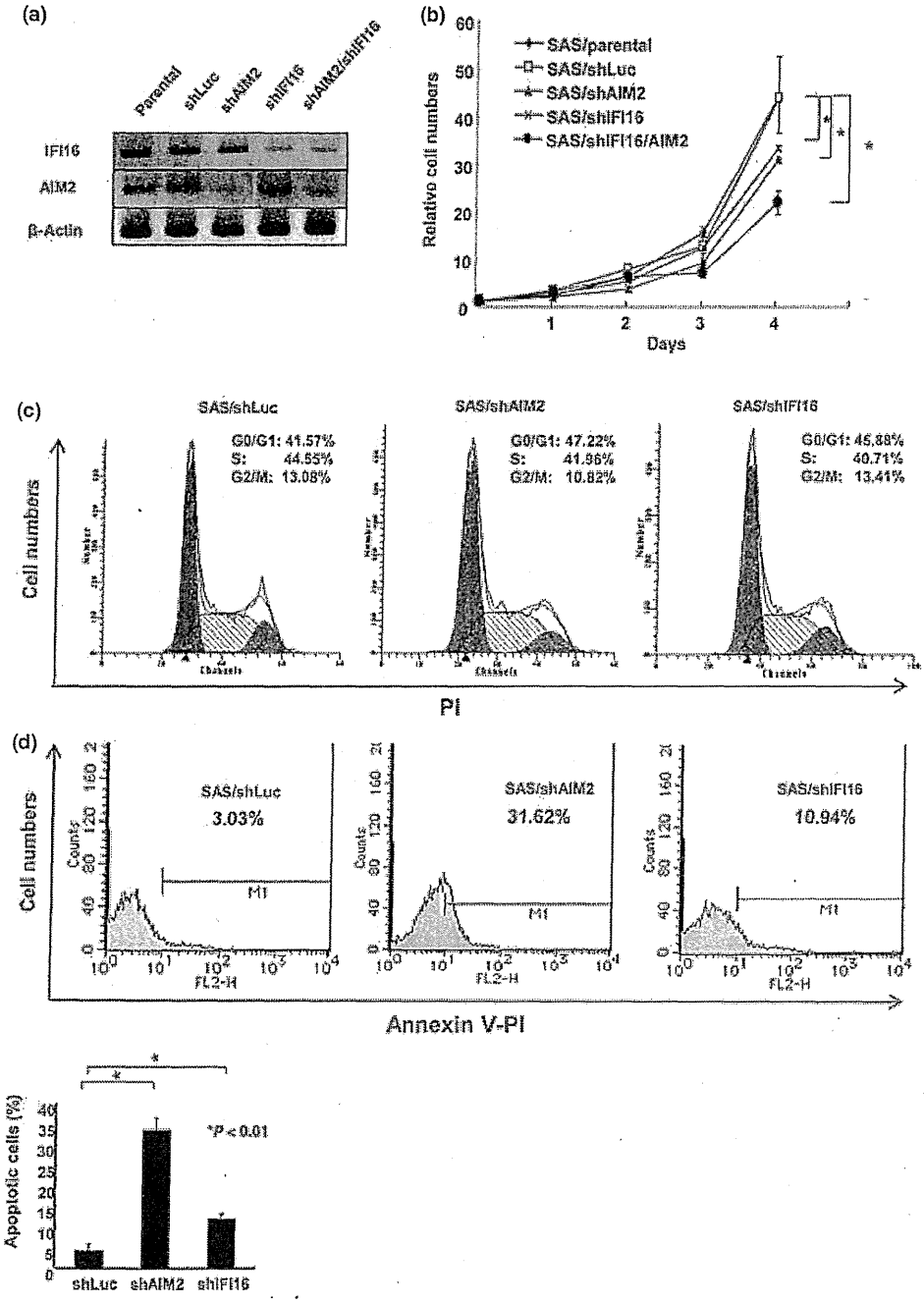

Fig. 2. *Effects of knockdown of AIM2 and IFI16 expression on the growth of OSCC cells.* (a) Retroviral constructs containing shRNA against AIM2 and/or IFI16 or luciferase (Luc) as a control were transfected into SAS cells. Forty-eight hours after transfection, ZsGreen-positive cells were sorted, and total RNA was extracted to analyze expression levels of AIM2 and IFI16 by RT-PCR. (b) The growth of sorted cells was analyzed with MTT. The data are shown as the mean ± SD of triplicate samples. The statistical analysis was performed using the Student's *t*-test (*$P < 0.01$). (c) Cell cycle phase distribution was analyzed by FACS with PIstaining. Each cycle phase distribution was analyzed by the cell recruited into the cell cycle. (d) The percentage of sorted cells undergoing apoptosis was quantitated by Annexin V staining and FACS. The lower bar graph shows the mean ± SD from three independent experiments. An asterisk indicates a statistically significant difference ($P < 0.01$). AIM2, absent in melanoma; IFI16, interferon-inducible 16.

shAIM2 was also confirmed by NF-κB-dependent luciferase reporter activity assay (Fig. 3f). The overexpression of IFI16 and AIM2 may enhance IκBα kinase activity and promote the degradation of IκBα and NF-κB activation, leading to the acceleration of cell growth in OSCC cells.

Restoration of p53 function inhibits constitutive NF-κB activation in OSCC cells. Studies have reported that the overexpression of HIN-200 proteins can decrease cell proliferation and block cell cycle progression at the G1-S phase transition.[14] It has been shown that IFI16-mediated growth arrest is partly dependent on

the function of p53.[15] Because a high frequency of mutations in p53 was noted in OSCC,[22] we determined whether p53 dysfunction results in abrogation of the growth suppressive effects of AIM2 and IFI16 in OSCC cells. Initially, we determined the expression and genomic alterations of p53 in eight OSCC cell lines. All cell lines showed p53 point mutations (Table S2-1, Doc. S2) and five (Ca9-22, HSC4, HSQ89, SAS and Sa3) expressed a detectable level of p53 protein, including a truncated form of p53 (Fig. 4a).[20,21] In primary OSCC samples, five out of 11 tumors had abnormally high expression levels and/or point mutations of p53 (data not shown) (Table S2-2). We introduced the wild-type p53 expression vector into the SAS cell line and confirmed that the expression of wild-type p53 decreased the growth rate of SAS cells (Fig. 4b,c). The percentage of Annexin V-positive cells significantly increased in wild-type p53-transfected cells (Fig. 4d), indicating that this p53-mediated growth suppression of SAS cells is associated with apoptosis.

It has been reported that p53 regulates glucose metabolism through the NF-κB pathway, and both basally expressed and genotoxicity-activated p53 inhibits the activity of IκB kinase and the transcriptional activity of NF-κB.[23] Therefore, we determined whether p53 could inhibit NF-κB activation in OSCC cells. A significant increase in the IκBα protein level and a decrease in phosphorylated IκBα were observed when SAS cells were transfected with wild-type p53 (Fig. 4e). Wild-type p53 also inhibited the basal NF-κB reporter activity of SAS cells (Fig. 4f). These data suggest that constitutive activation of the NF-κB pathway in OSCC is partly due to a loss of p53 function.

The overexpression AIM2 and IFI16 synergistically promotes cell growth only in the absence of functional p53. To determine whether a lack of functional p53 is associated with the growth-promoting effect of AIM2 and IFI16 in OSCC cells, we transfected human lung cancer H1299 cells, which lack endogenous p53,[24] with various combinations of the AIM2, IFI16 and p53 expression vectors. The transfection of AIM2, IFI16, or p53 alone had no significant effect on the growth rate of H1299 cells (Fig. 5a,b). However, co-transfection of AIM2 and IFI16 strongly promoted cell proliferation with increased IκBα phosphorylation. Strikingly, the growth-promoting effect of AIM2 and IFI16 was abrogated in the presence of wild-type p53. To further confirm these results, we performed cell proliferation assays using the human mammary tumor cell line MCF-7 expressing wild-type p53, which has been used to study the role of IFI16 in p53-dependent apoptosis.[25] Transfection with either or both of the AIM2 and IFI16 expression vectors retarded the growth rate of MCF-7 cells. The shRNA inhibition of p53 expression caused a slight increase in cell growth rate (Fig. 5c,d). Importantly, co-transfection of AIM2 and IFI16 with a shRNA expression vector for p53 led to an approximately two-fold higher proliferation rate with significant upregulation of phosphorylated IκBα. Thus, the simultaneous high expression of AIM2 and IFI16 confers a proliferative advantage in cells with functionally inactive p53, in part, through the activation of NF-κB signaling.

Finally, we examined whether co-expression of both AIM2 and IFI16 can activate NF-κB in an OSCC cell line. Very low expression levels of AIM2 and IFI16 and a low level of NF-κB

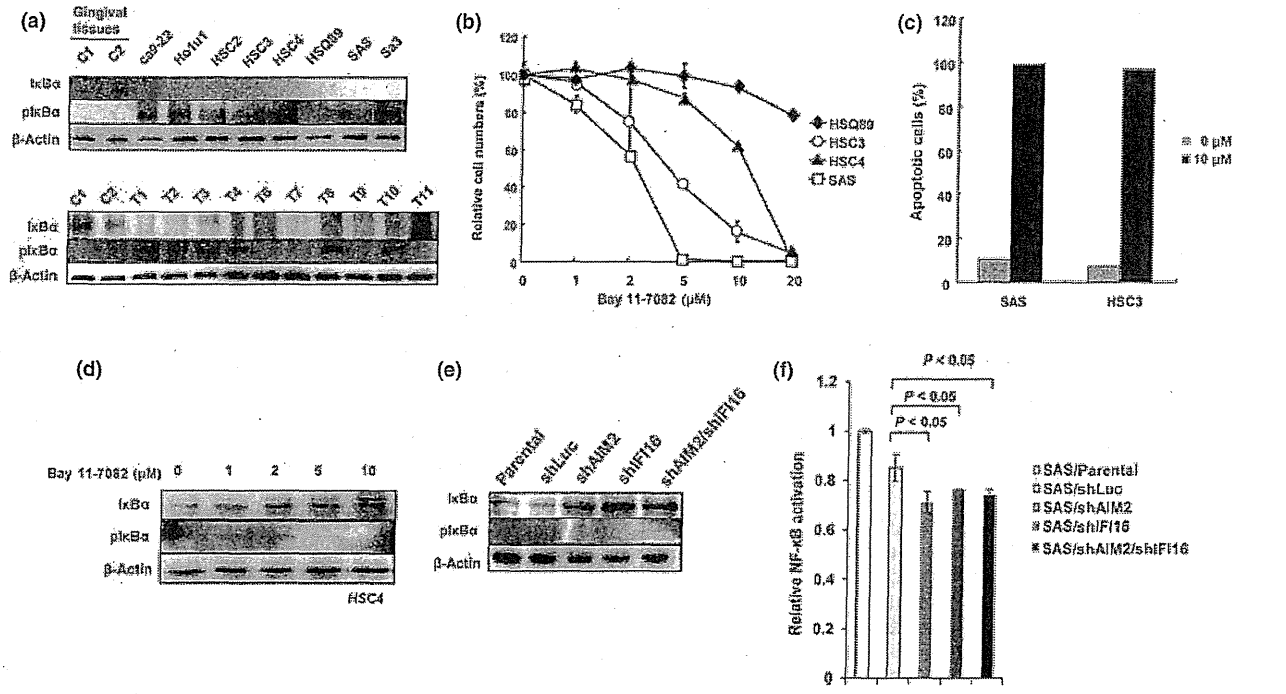

Fig. 3. Activation of NF-κB signaling in oral squamous cell carcinoma (OSCC). (a) The levels of total and phosphorylated (Ser32/36) inhibitor of kappa B alpha (IκBα) were examined in two normal gingival tissue samples, eight OSCC cell lines (Ca9-22, Ho1u1, HSC2, HSC3, HSC4, HSQ89, SAS and Sa3) and 10 OSCC primary tumors by Western blot analysis. (b) Four OSCC cell lines were treated with various concentrations of Bay 11-7082 for 48 h, and viable cell numbers were counted by MTT assay. The results are shown as percentages of the values obtained from the control Bay 11-7082-free culture. The data are shown as the means ± SD of triplicate samples. (c) The percentage of apoptotic cells was measured by FACS after Annexin V/PI staining in untreated and 10-μM Bay 11-7082-treated SAS and HSC3 cell lines at 48 h. (d) Levels of phosphorylated IκBα and total IκBα in the HSC4 cell line treated with the indicated concentration of Bay 11-7082 for 48 h were examined by Western blot analysis. (e) The SAS cell transfectants described in Figure 2 were examined for the levels of phosphorylated IκBα and total IκBα by Western blot analysis. (f) The SAS cell transfectants were co-transfected with the NF-κB–Luc reporter and an internal control Renilla luciferase (pRL-TK) plasmid. After 36 h, luciferase activities were measured with a dual-luciferase reporter assay system. The data are shown as mean ± SD of triplicate transfections, and statistical analysis used the Student's *t*-test. NF-κB, nuclear factor·kappa-light-chain-enhancer of activated B cells.

doi: 10.1111/j.1349-7006.2012.02211.x

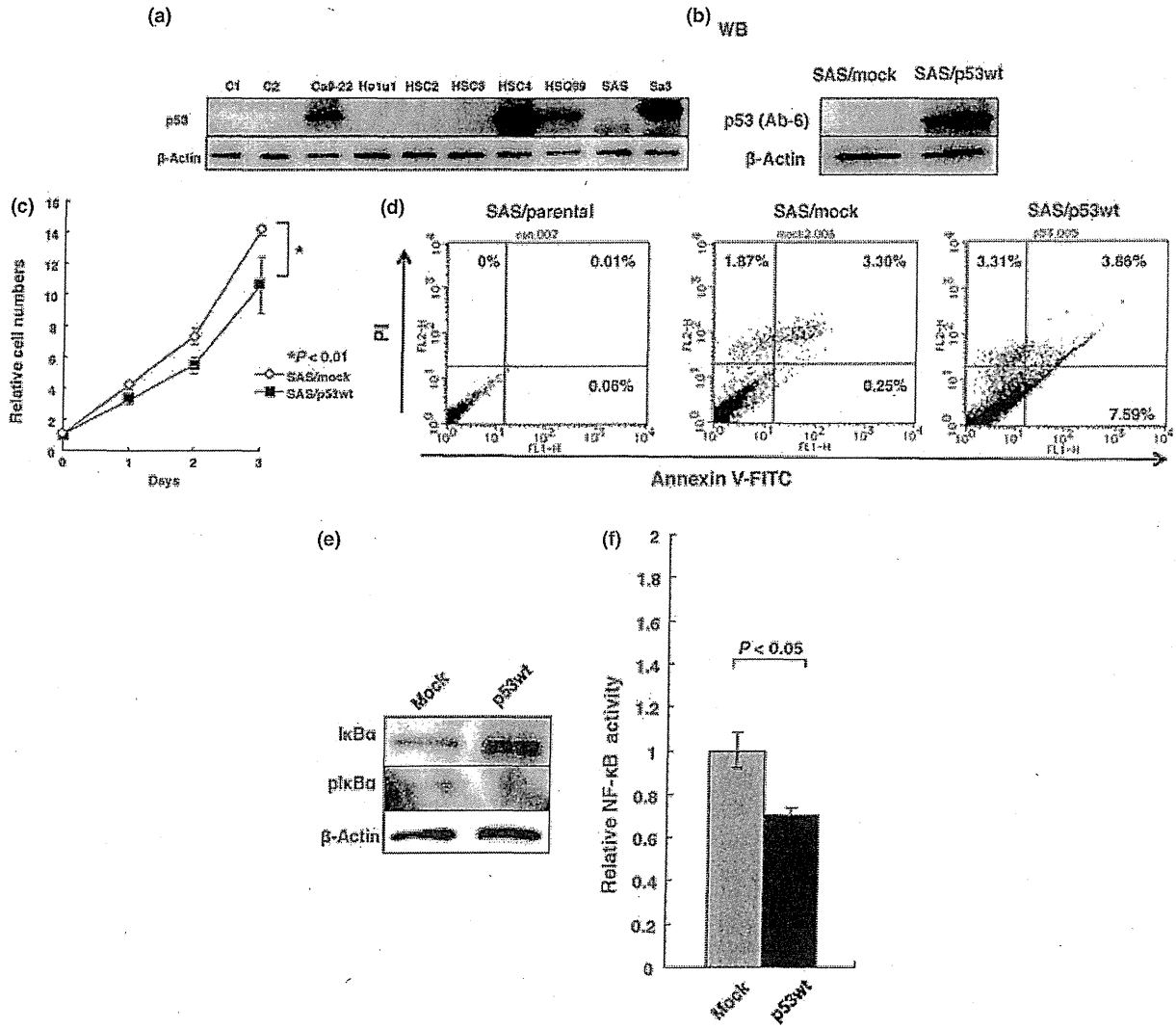

Fig. 4. Function of p53 is inhibited in oral squamous cell carcinoma (OSCC) cells. (a) Detection of p53 protein levels in two normal gingival tissues and in eight OSCC cell lines (Ca9-22, Ho1u1, HSC2, HSC3, HSC4, HSQ89, SAS and Sa3) by Western blot analysis. (b) SAS cell lines stably transfected with either empty vector or wild-type p53 expression vector (FLAG-p53wt) were examined for expression of p53 by Western blot using an anti-p53 antibody (Ab-6). (c) Transfectants were subjected to cell growth analysis using the MTT assay. The data are shown as the mean ± SD of triplicate samples. The statistical analysis was done using the Student's *t*-test. (d) The percentage of apoptotic cells was quantified by Annexin-V/PI staining. (e) Control vector and p53 transfectants were examined for levels of phosphorylated inhibitor of kappa B alpha (IκBα) and total IκBα by Western blot analysis. (f) The cells were co-transfected with NF-κB–Luc and pRL-TK. After 36 h, luciferase activities were measured. The data are presented as in Figure 3(f). NF-κB, nuclear factor kappa-light-chain-enhancer of activated B cells.

activation were found in HSQ89 with p53 mutation. Although transfection of either AIM2 or IFI16 alone did not have a significant effect on NF-κB activation and cell growth, co-transfection of AIM2 and IFI16 resulted in accelerated cell proliferation, a decrease in total IκBα, and an increase in phosphorylated IκBα (Fig. 5e,f). This result suggests that co-expression of AIM2 and IFI16 activates NF-κB signaling in OSCC cells. Taken together, these results suggest that co-expression of AIM2 and IFI16 can promote cell proliferation through activation of NF-κB signaling pathway in the absence of p53.

Discussion

The oral cavity contains some of the most varied and extensive flora in the entire human body. A member of a group of DNA-based viruses, HPV infects the skin and mucous membranes within the human body. Infection with HPV 16 and 18 increases the risk of oral cavity cancer and oropharyngeal cancer.[11] Because the interferon-inducible *AIM2* and *IFI16* genes act as innate immune sensors for cytosolic double-stranded DNA,[12,13] the expression of AIM2 and/or IFI16 might be activated by recurrent infections in the oral cavity. In this study, we showed that constitutive high expression levels of *AIM2* and *IFI16*, along with other interferon-inducible genes, were associated with genomic alterations in OSCC. Upregulation of a series of interferon-inducible genes and enhancement of interferon-signaling pathways has previously been reported in OSCC by protein expression analysis using tandem mass spectrometry or by mRNA expression profile analysis using a DNA microarray.[26,27] The expression of the interferon-inducible gene is an important characteristic of OSCC. Moreover, OSCC cells were shown to become resistant to IFN-β-mediated inhibition of cell growth.[26] The constitutive expression of the interferon-inducible genes may affect the development of OSCC, and the expres-

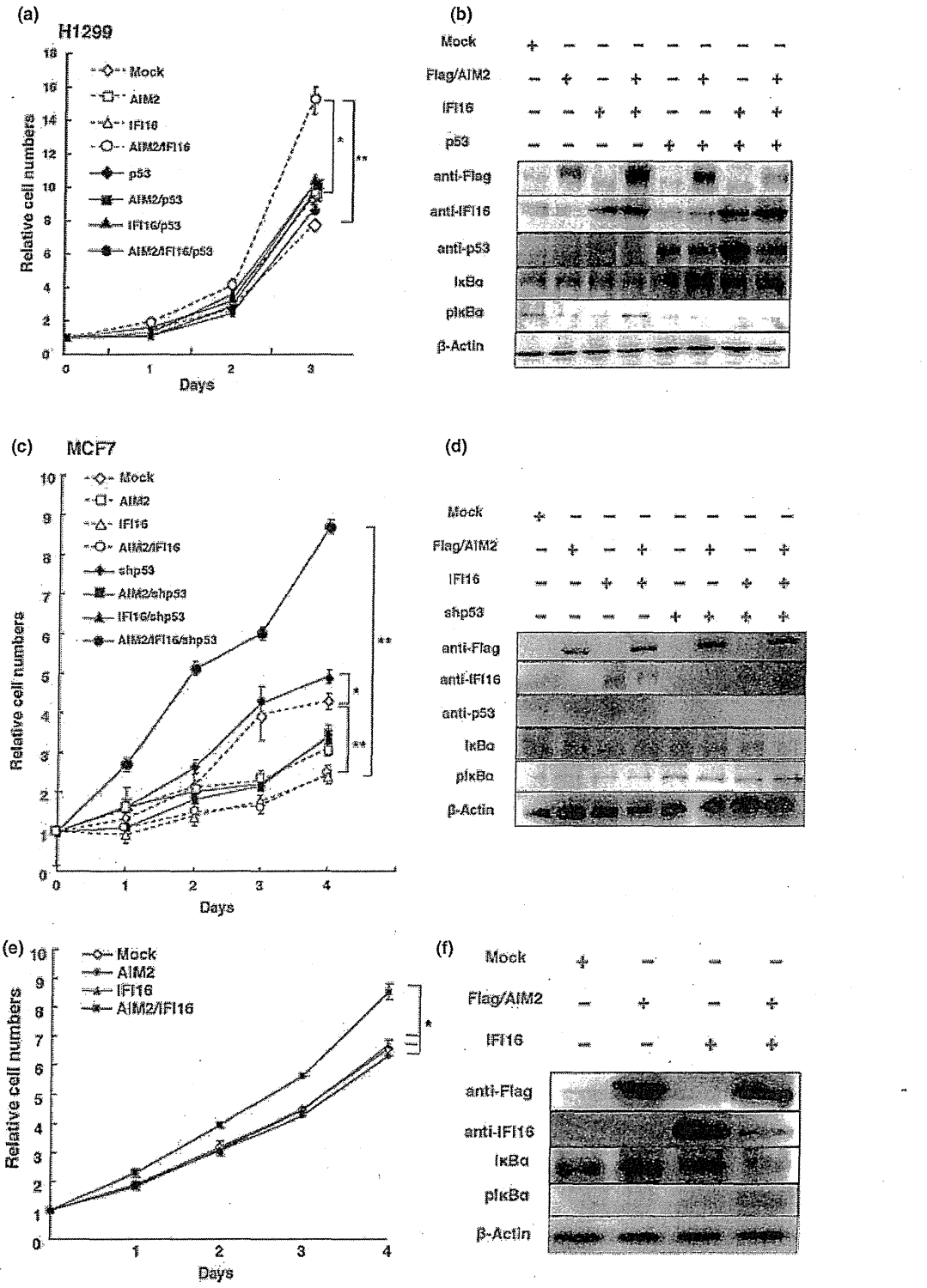

Fig. 5. Expression of AIM2 and IFI16 confers growth-stimulating effects on transformed cells in the absence of wild-type p53. (a) The growth of human lung cancer H1299 cells after transfection with various combinations of AIM2, IFI16 and wild-type p53 (SN3-p53wt) expression vectors was examined by MTT assay. The data are shown as the mean ± SD of triplicate samples. The statistical analysis was performed using the Student's *t*-test (*$P < 0.05$; **$P < 0.01$). (b) Western blot analysis of extracts from untransfected or transfected H1299 cells described in panel (a) at 48 h. (c) The growth of human mammary tumor MCF7 cells after transfection with various combinations of the AIM2, IFI16 and shp53 expression vectors was examined by MTT assay. The data are shown as the mean ± SD of triplicate samples. The statistical analysis was performed using the Student's *t*-test (*$P < 0.05$; **$P < 0.01$). (d) Western blot analysis of extracts from untransfected or transfected MCF7 cells described in panel (c) at 48 h. (e) The growth of HSQ89 cells after transfection with AIM2 and/or IFI16. (f) Western blot analysis of extracts from untransfected or transfected HSQ89 cells described in panel (e) at 48 h. AIM2, absent in melanoma; IκBα, inhibitor of kappa B alpha; IFI16, interferon-inducible 16.

doi: 10.1111/j.1349-7006.2012.02211.x

sion of a subset of the interferon-inducible genes may arise as a result of genomic alterations.

Although the *AIM2* and *IFI16* genes were thought to be tumor suppressors in a series of cancers, high expression levels of AIM2 and IFI16 enhanced the cell growth and prevented apoptosis in OSCC. In normal aged human cells, increased levels of the IFI16 protein reportedly contribute to senescence-associated cell growth arrest partly through the p53/p21CIP1 and Rb/E2F pathway and upregulation of IFI16 expression by p53. This is a part of a component of the positive feedback loop between p53 and IFI16.[28] Because the loss of p53 and/or IFI16 function in cells has been suggested to contribute to defects in cellular senescence-associated cell growth arrest, we speculate that dysregulated IFI16 function together with the loss of p53 function can contribute to the development of OSCC. This study demonstrated that the co-expression of AIM2 and IFI16 synergistically activates NF-κB signaling, and the activation of NF-κB in OSCC is also dependent on p53 inactivation. Future studies will determine the precise activation mechanisms of NF-κB signaling and/or the transcriptional activity of IFI16 in OSCC with inactivated p53.

Disclosure Statement

The authors have no conflict of interest to declare.

Abbreviations

AIM2	absent in melanoma 2
HIN-200	hematopoietic interferon-inducible nuclear proteins with a 200-amino-acid repeat
HPV	human papillomavirus
IFI	interferon-inducible
IFN	interferon
IκBα	inhibitor of kappa B alpha
NF-κB	nuclear factor kappa-light-chain-enhancer of activated B cells
OSCC	oral squamous cell carcinoma
SNP	single-nucleotide polymorphism

References

1 Shah JP, Singh B. Keynote comment: why the lack of progress for oral cancer? *Lancet Oncol* 2006; **7**: 356–7.
2 Gibson MK, Forastiere AA. Reassessment of the role of induction chemotherapy for head and neck cancer. *Lancet Oncol* 2006; **7**: 565–74.
3 Perez-Sayans M, Somoza-Martin JM, Barros-Angueira F, Reboiras-Lopez MD, Gandara Rey JM, Garcia-Garcia A. Genetic and molecular alterations associated with oral squamous cell cancer (Review). *Oncol Rep* 2009; **22**: 1277–82.
4 Rogers SJ, Harrington KJ, Rhys-Evans P, P OC, Eccles SA. Biological significance of c-erbB family oncogenes in head and neck cancer. *Cancer Metastasis Rev* 2005; **24**: 47–69.
5 Rousseau A, Lim MS, Lin Z, Jordan RC. Frequent cyclin D1 gene amplification and protein overexpression in oral epithelial dysplasias. *Oral Oncol* 2001; **37**: 268–75.
6 Reed AL, Califano J, Cairns P *et al.* High frequency of p16 (CDKN2/MTS-1/INK4A) inactivation in head and neck squamous cell carcinoma. *Cancer Res* 1996; **56**: 3630–3.
7 Choi S, Myers JN. Molecular pathogenesis of oral squamous cell carcinoma: implications for therapy. *J Dent Res* 2008; **87**: 14–32.
8 Sisk EA, Soltys SG, Zhu S, Fisher SG, Carey TE, Bradford CR. Human papillomavirus and p53 mutational status as prognostic factors in head and neck carcinoma. *Head Neck* 2002; **24**: 841–9.
9 Min BM, Baek JH, Shin KH, Gujuluva CN, Cherrick HM, Park NH. Inactivation of the p53 gene by either mutation or HPV infection is extremely frequent in human oral squamous cell carcinoma cell lines. *Eur J Cancer B Oral Oncol* 1994; **30B**: 338–45.
10 Boyer SN, Wazer DE, Band V. E7 protein of human papilloma virus-16 induces degradation of retinoblastoma protein through the ubiquitin-proteasome pathway. *Cancer Res* 1996; **56**: 4620–4.
11 Feller L, Wood NH, Khammissa RA, Lemmer J. Human papillomavirus-mediated carcinogenesis and HPV-associated oral and oropharyngeal squamous cell carcinoma. Part 1: human papillomavirus-mediated carcinogenesis. *Head Face Med* 2010; **6**: 14.
12 Unterholzner L, Keating SE, Baran M *et al.* IFI16 is an innate immune sensor for intracellular DNA. *Nat Immunol* 2010; **11**: 997–1004.
13 Fernandes-Alnemri T, Yu JW, Datta P, Wu J, Alnemri ES. AIM2 activates the inflammasome and cell death in response to cytoplasmic DNA. *Nature* 2009; **458**: 509–13.
14 Asefa B, Klarmann KD, Copeland NG, Gilbert DJ, Jenkins NA, Keller JR. The interferon-inducible p200 family of proteins: a perspective on their roles in cell cycle regulation and differentiation. *Blood Cells Mol Dis* 2004; **32**: 155–67.
15 Ludlow LE, Johnstone RW, Clarke CJ. The HIN-200 family: more than interferon-inducible genes? *Exp Cell Res* 2005; **308**: 1–17.
16 Liao JC, Lam R, Brazda V *et al.* Interferon-inducible protein 16: insight into the interaction with tumor suppressor p53. *Structure* 2011; **19**: 418–29.
17 Chen IF, Ou-Yang F, Hung JY *et al.* AIM2 suppresses human breast cancer cell proliferation in vitro and mammary tumor growth in a mouse model. *Mol Cancer Ther* 2006; **5**: 1–7.
18 Toruner GA, Ulger C, Alkan M *et al.* Association between gene expression profile and tumor invasion in oral squamous cell carcinoma. *Cancer Genet Cytogenet* 2004; **154**: 27–35.
19 Zhong LP, Zhao SF, Chen GF, Ping FY, Xu ZF, Hu JA. Increased levels of CK19 mRNA in oral squamous cell carcinoma tissue detected by relative quantification with real-time polymerase chain reaction. *Arch Oral Biol* 2006; **51**: 1112–9.
20 Ding YM, Dong JH, Chen LL, Zhang HD. Increased expression of galectin-1 is associated with human oral squamous cell carcinoma development. *Oncol Rep* 2009; **21**: 983–7.
21 Azzimonti B, Pagano M, Mondini M *et al.* Altered patterns of the interferon-inducible gene IFI16 expression in head and neck squamous cell carcinoma: immunohistochemical study including correlation with retinoblastoma protein, human papillomavirus infection and proliferation index. *Histopathology* 2004; **45**: 560–72.
22 Martin-Ezquerra G, Salgado R, Toll A *et al.* Multiple genetic copy number alterations in oral squamous cell carcinoma: study of MYC, TP53, CCDN1, EGFR and ERBB2 status in primary and metastatic tumours. *Br J Dermatol* 2010; **163**: 1028–35.
23 Kawauchi K, Araki K, Tobiume K, Tanaka N. p53 regulates glucose metabolism through an IKK-NF-kappaB pathway and inhibits cell transformation. *Nat Cell Biol* 2008; **10**: 611–8.
24 Takahashi T, Takahashi T, Suzuki H *et al.* The p53 gene is very frequently mutated in small-cell lung cancer with a distinct nucleotide substitution pattern. *Oncogene* 1991; **6**: 1775–8.
25 Fujiuchi N, Aglipay JA, Ohtsuka T *et al.* Requirement of IFI16 for the maximal activation of p53 induced by ionizing radiation. *J Biol Chem* 2004; **279**: 20339–44.
26 Chi LM, Lee CW, Chang KP *et al.* Enhanced interferon signaling pathway in oral cancer revealed by quantitative proteome analysis of microdissected specimens using 16O/18O labeling and integrated two-dimensional LC-ESI-MALDI tandem MS. *Mol Cell Proteomics* 2009; **8**: 1453–74.
27 Chen C, Mendez E, Houck J *et al.* Gene expression profiling identifies genes predictive of oral squamous cell carcinoma. *Cancer Epidemiol Biomarkers Prev* 2008; **17**: 2152–62.
28 Song LL, Alimirah F, Panchanathan R, Xin H, Choubey D. Expression of an IFN-inducible cellular senescence gene, IFI16, is up-regulated by p53. *Mol Cancer Res* 2008; **6**: 1732–41.

Supporting Information

Additional Supporting Information may be found in the online version of this article:

Fig. S1. Genome-wide measurement of DNA copy number alterations in oral squamous cell carcinoma (OSCC).

Fig. S2. IFI16 and AIM2 are upregulated in oral squamous cell carcinoma (OSCC).

Fig. S3. Downregulation of either AIM2 or IFI16 expression decreases the growth rate of HSC4 cells.

Fig. S4. Downregulation of either AIM2 or IFI16 expression increases apoptosis in SAS cells.

Fig. S5. Caspase-1 is not activated in oral squamous cell carcinoma cells.

Fig. S6. Treatment with Bay 11-7082 induced apoptosis in oral squamous cell carcinoma (OSCC) cells.

Table S1. Summary of DNA copy number aberrations in 28 oral squamous cell carcinoma (OSCC) tumors.

Table S2. *p53* status in primary oral squamous cell carcinoma tumors (OSCC) and cell lines.

Data S1. Materials and methods.

Data S2. Additional references in Table S2 and Data S1.

Please note: Wiley-Blackwell are not responsible for the content or functionality of any supporting materials supplied by the authors. Any queries (other than missing material) should be directed to the corresponding author for the article.

doi: 10.1111/j.1349-7006.2012.02211.x

Leukemia (2012) 26, 1238–1246

www.nature.com/leu

ORIGINAL ARTICLE

Clinical significance of CADM1/TSLC1/IgSF4 expression in adult T-cell leukemia/lymphoma

S Nakahata[1], Y Saito[1], K Marutsuka[2], T Hidaka[3], K Maeda[3,4], K Hatakeyama[5], T Shiraga[1,6], A Goto[1], N Takamatsu[1], Y Asada[5], A Utsunomiya[7], A Okayama[8], Y Kubuki[3], K Shimoda[3], Y Ukai[9], G Kurosawa[9] and K Morishita[1]

Cell adhesion molecule 1 (CADM1/TSLC1) was recently identified as a novel cell surface marker for adult T-cell leukemia/lymphoma (ATLL). In this study, we developed various antibodies as diagnostic tools to identify CADM1-positive ATLL leukemia cells. In flow cytometric analysis, the percentages of $CD4^+CADM1^+$ double-positive cells correlated well with both the percentages of $CD4^+CD25^+$ cells and with abnormal lymphocytes in the peripheral blood of patients with various types of ATLL. Moreover, the degree of $CD4^+CADM1^+$ cells over 1% significantly correlated with the copy number of the human T-lymphotropic virus type 1 (HTLV-1) provirus in the peripheral blood of HTLV-1 carriers and ATLL patients. We also identified a soluble form of CADM1 in the peripheral blood of ATLL patients, and the expression levels of this form were correlated with the levels of soluble interleukin 2 receptor alpha. Moreover, lymphomas derived from ATLL were strongly and specifically stained with a CADM1 antibody. Thus, detection of $CD4^+CADM1^+$ cells in the peripheral blood, measurement of serum levels of soluble CADM1 and immunohistochemical detection of CADM1 in lymphomas would be a useful set of markers for disease progression in ATLL and may aid in both the early diagnosis and measurement of treatment efficacy for ATLL.

Leukemia (2012) **26**, 1238–1246; doi:10.1038/leu.2011.379; published online 6 January 2012

Keywords: CADM1/IgSF4/TSLC1; ATLL

INTRODUCTION

Adult T-cell leukemia/lymphoma (ATLL) results from infection with human T-lymphotropic virus type 1 (HTLV-1).[1,2] Following HTLV-1 infection, 2.1 to 6.6% of HTLV-1 carriers will develop ATLL, and most of the ATLL patients will die within a year.[3] An estimated 10–20 million people worldwide are infected with HTLV-1, and HTLV-1 is endemic in southwestern Japan, the island of Kyushu, Africa, the Caribbean Islands and South America.[4] ATLL cells are mainly derived from activated helper T cells with the $CD3^+$, $CD4^+$, $CD8^-$ and $CD25^+$ (also known as interleukin 2 receptor alpha (IL-2Rα)) cell surface markers.[2] A fraction of ATLL cases have been shown to also express forkhead box P3 (*FOXP3*), which is a master gene for regulatory T cells (T-reg), suggesting that some cases of ATLL may originate from HTLV-1-infected T-reg cells.[5,6] For diagnosis, identification of mono- or oligoclonal provirus integration events by Southern blot analysis is one of the definitive markers for ATLL. In addition to viral integration, ATLL cells with multi-lobulated nuclei (called 'flower cells') have been frequently seen in leukemia cells in the peripheral blood of ATLL patients. Hypercalcemia and high levels of either serum lactate dehydrogenase (LDH) or soluble IL-2Rα (sIL-2Rα) have been found to be unfavorable markers for ATLL; however, these markers are not specific for the diagnosis of ATLL.[7,8]

The developmental steps of ATLL after HTLV-1 infection have remained obscure for 30–40 years. HTLV-1 Tax is thought to be an important viral protein that functions in the maintenance of HTLV-1-infected lymphocytes;[9,10] however, expression of Tax protein was not detected in over 70% of ATLL cases because of genomic deletion and/or DNA methylation.[11–14] Recently, HTLV-1 basic leucine zipper (HBZ) was found to be constitutively expressed in ATLL cells and was shown to interact with JUN and CREB2 to regulate Tax expression.[15,16] HBZ also promotes $CD4^+$ T-cell proliferation in transgenic mice;[16] therefore, HBZ has important roles and functions not only in maintaining the virus life cycle but also in the maintenance of the HTLV-1-infected cells that contribute to disease pathogenesis. Although HBZ is expressed in the majority of ATLL cells, only 5% of HTLV-1 carriers develop ATLL, suggesting that additional factors besides viral infection are required for the development of ATLL.

To identify additional pathogenic factors or novel surface markers for ATLL, we collected gene expression profiles for acute-type ATLL. Using a comprehensive DNA microarray gene expression analysis, we recently demonstrated that cell adhesion molecule 1 (CADM1/TSLC1/IgSF4) is a novel cell surface maker for ATLL.[17] CADM1 was initially isolated as a tumor suppressor for lung cancers by genomic analysis. CADM1 expression is reduced in a variety of cancers by promoter methylation and is associated with poor prognosis and enhanced metastatic potential.[18] By contrast, we identified that high expression of CADM1 has an important role in enhanced cell–cell adhesion to the vascular endothelium, tumor growth and the organ infiltration of ATLL cells.[19]

In this study, we developed various antibodies for CADM1 to be used as diagnostic tools for identifying ATLL leukemia cells.

[1]Division of Tumor and Cellular Biochemistry, Department of Medical Sciences, Faculty of Medicine, University of Miyazaki, Miyazaki, Japan; [2]Pathology Division, University of Miyazaki Hospital, Miyazaki, Japan; [3]Department of Gastroenterology and Hematology, Faculty of Medicine, Miyazaki University, Miyazaki, Japan; [4]Department of Internal Medicine, Miyakonojo National Hospital, Miyazaki, Japan; [5]Department of Pathology, Faculty of Medicine, University of Miyazaki, Miyazaki, Japan; [6]Department of Foods and Human Nutrition, Faculty of Human Life Sciences, Notre Dame Seishin University, Okayama, Japan; [7]Department of Hematology, Imamura Bun-in Hospital, Kagoshima, Japan; [8]Department of Rheumatology, Infectious Diseases and Laboratory Medicine, University of Miyazaki, Miyazaki, Japan and [9]Division of Antibody Project, Institute for Comprehensive Medical Science, Fujita Health University, Aichi, Japan. Correspondence: Professor K Morishita, Division of Tumor and Cellular Biochemistry, Department of Medical Science, Faculty of Medicine, University of Miyazaki, 5200 Kihara, Kiyotake, Miyazaki 889-1692, Japan.
E-mail: kmorishi@med.miyazaki-u.ac.jp
Received 14 April 2011; revised 24 November 2011; accepted 29 November 2011; published online 6 January 2012